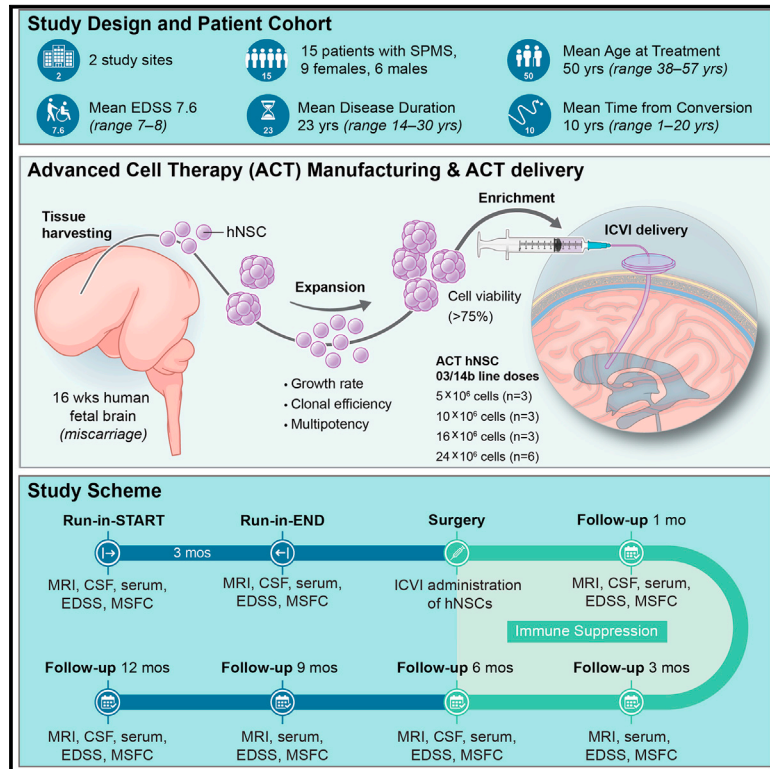


Phase I clinical trial of intracerebroventricular transplantation of allogeneic neural stem cells in people with progressive multiple sclerosis

Graphical abstract



Authors

Maurizio A. Leone, Maurizio Gelati, Daniela C. Profico, ..., Luca Peruzzotti-Jametti, Stefano Pluchino, Angelo L. Vescovi

Correspondence

spp24@cam.ac.uk (S.P.), angelo.vescovi@unimib.it (A.L.V.)

In brief

Leone, Gelati, and colleagues assessed the intracerebroventricular injection (ICVI) of allogeneic human neural stem/progenitor cells (hNSCs) for the treatment of progressive multiple sclerosis. The ICVI of highly purified and stable hNSC lines displays an optimal feasibility, safety, and tolerability profile.

Highlights

- An advanced therapy with neural stem/progenitor cells (NSCs) is feasible in humans
- NSC grafts are tolerated by people with secondary progressive multiple sclerosis
- Doses of the injected NSCs inversely correlate with parenchymal brain volume changes
- Time- and dose-dependent increase of CSF acyl-carnitines and fatty acids is described

Clinical and Translational Report

Phase I clinical trial of intracerebroventricular transplantation of allogeneic neural stem cells in people with progressive multiple sclerosis

Maurizio A. Leone,^{1,12} Maurizio Gelati,^{1,12} Daniela C. Profico,^{1,12} Claudio Gobbi,^{2,3} Emanuele Pravatà,^{2,3,4} Massimiliano Copetti,¹ Carlo Conti,⁸ Lucrezia Abate,¹ Luigi Amoroso,¹ Francesco Apollo,¹ Rosario F. Balzano,⁴ Iliaria Bicchi,^{1,9} Massimo Carella,¹ Alessandro Ciampini,⁹ Carlo Colosimo,⁹ Paola Crociani,¹ Giada D'Aloisio,¹ Pietro Di Viesti,¹ Daniela Ferrari,⁷ Danilo Fogli,¹ Andrea Fontana,¹ Domenico Frondizi,⁹ Valentina Grespi,^{1,9} Jens Kuhle,¹⁰ Antonio Laborante,¹ Ivan Lombardi,⁷ Gianmarco Muzi,⁹ Francesca Paci,⁹ Giuliana Placentino,¹ Teresa Popolizio,¹ Claudia Ricciolini,^{1,9} Simonetta Sabatini,⁹ Giada Silveri,¹ Cristina Spera,⁹ Daniel Stephenson,⁸ Giuseppe Stipa,⁹ Elettra Tinella,⁹ Michele Zarelli,¹ Chiara Zecca,^{2,3} Yendri Ventura,¹¹ Angelo D'Alessandro,⁸ Luca Peruzzotti-Jametti,^{5,6} Stefano Pluchino,^{5,*} and Angelo L. Vescovi^{1,7,13,*}

¹IRCCS Casa Sollievo della Sofferenza, Viale Cappuccini 1, San Giovanni Rotondo, 71013 Foggia, Italy

²Multiple Sclerosis Centre (MSC), Department of Neurology, Neurocentre of Southern Switzerland, EOC, 6900 Lugano, Switzerland

³Faculty of Biomedical Sciences, Università della Svizzera Italiana (USI), 6900 Lugano, Switzerland

⁴Department of Neuroradiology, Neurocentre of Southern Switzerland, EOC, 6900 Lugano, Switzerland

⁵Department of Clinical Neurosciences and NIHR Biomedical Research Centre, University of Cambridge, CB2 0QQ Cambridge, UK

⁶Department of Metabolism, Digestion and Reproduction, Imperial College London, London, UK

⁷Department of Biotechnology and Biosciences, University of Milano-Bicocca, Piazza della Scienza 2, 20126 Milan, Italy

⁸Department of Biochemistry and Molecular Genetics, University of Colorado Anschutz Medical Campus, 12801 East 17th A - L18-9118, Aurora, CO, USA

⁹AOSP Santa Maria, via Tristano di Joannuccio 1, 05100 Terni, Italy

¹⁰Department of Neurology, University Hospital Basel, and University of Basel, Basel, Switzerland

¹¹Abu Dhabi Stem Cell Centre, Abu Dhabi, United Arab Emirates

¹²These authors contributed equally

¹³Lead contact

*Correspondence: spp24@cam.ac.uk (S.P.), angelo.vescovi@unimib.it (A.L.V.)

<https://doi.org/10.1016/j.stem.2023.11.001>

SUMMARY

We report the analysis of 1 year of data from the first cohort of 15 patients enrolled in an open-label, first-in-human, dose-escalation phase I study (ClinicalTrials.gov: NCT03282760, EudraCT2015-004855-37) to determine the feasibility, safety, and tolerability of the transplantation of allogeneic human neural stem/progenitor cells (hNSCs) for the treatment of secondary progressive multiple sclerosis.

Participants were treated with hNSCs delivered via intracerebroventricular injection in combination with an immunosuppressive regimen. No treatment-related deaths nor serious adverse events (AEs) were observed. All participants displayed stability of clinical and laboratory outcomes, as well as lesion load and brain activity (MRI), compared with the study entry. Longitudinal metabolomics and lipidomics of biological fluids identified time- and dose-dependent responses with increased levels of acyl-carnitines and fatty acids in the cerebrospinal fluid (CSF).

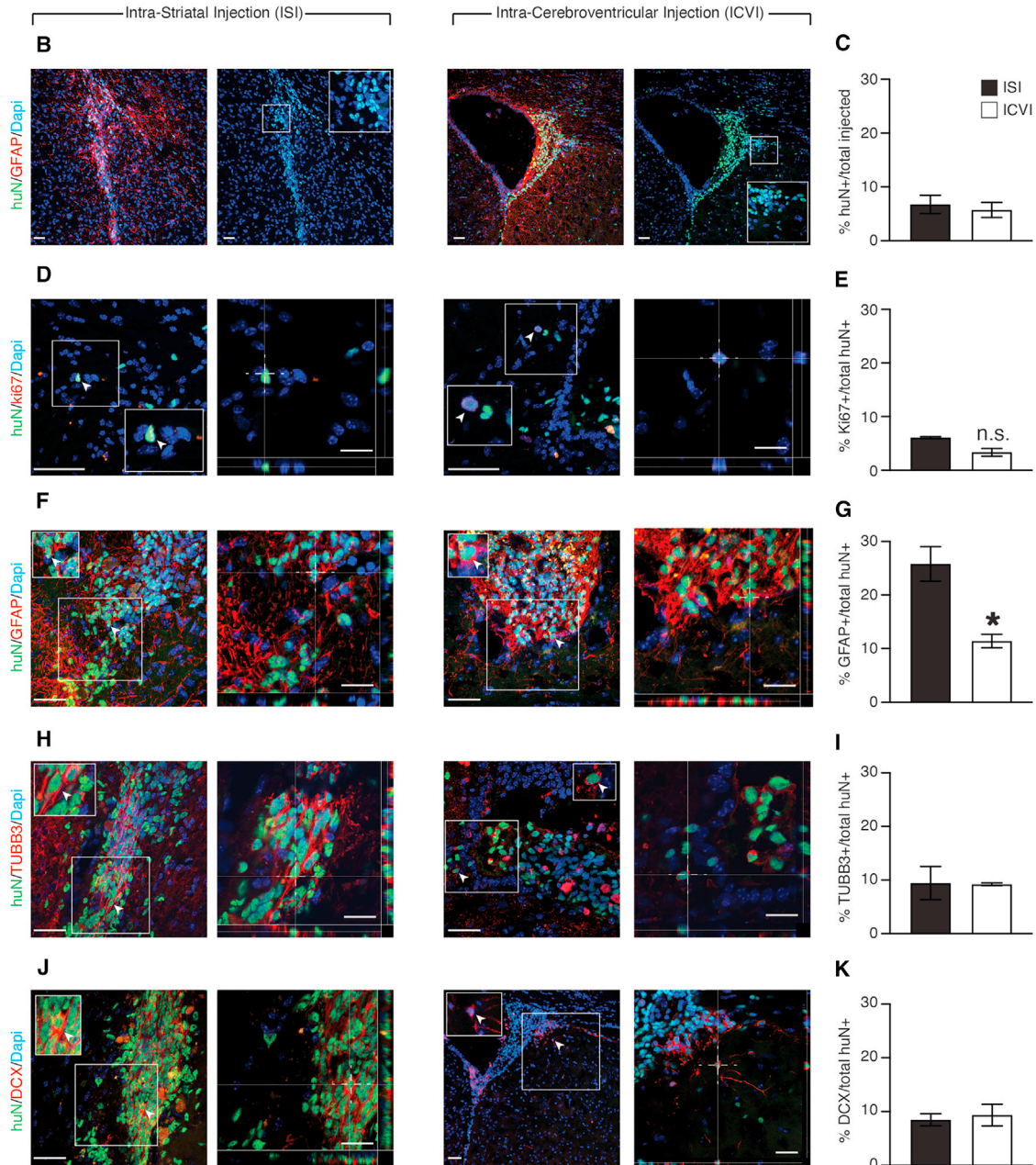
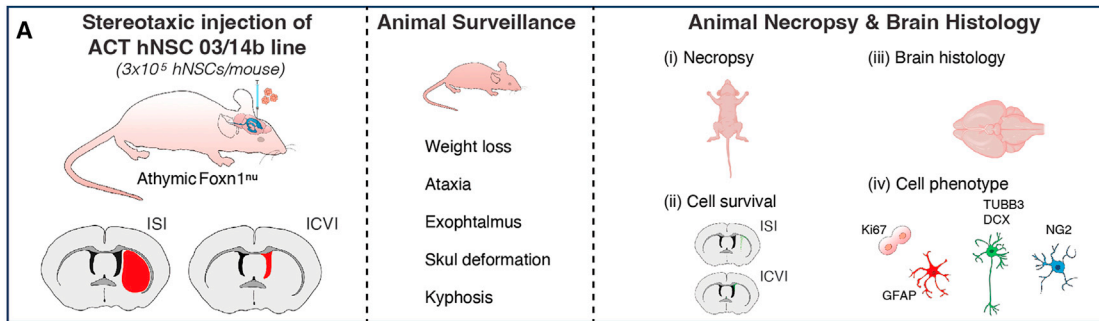
The absence of AEs and the stability of functional and structural outcomes are reassuring and represent a milestone for the safe translation of stem cells into regenerative medicines.

INTRODUCTION

Multiple sclerosis (MS) is a chronic neuroinflammatory condition that affects over 2 million people worldwide.¹ Although progress toward the development of disease-modifying therapies (DMTs) has made a substantial impact on the severity and frequency of MS relapses,² two-thirds of patients with MS still transition into a debilitating secondary progressive phase of disease within 25–30 years of diagnosis.³ Most DMTs have indeed shown only a

marginal effect on disease progression and MS-associated rates of global and regional brain volume loss.^{4,5} Ultimately, patients with secondary progressive MS (SPMS) experience a gradual, increasing, and irreversible accumulation of disability for which there is no treatment.⁶

Aiming to develop recommendations to accelerate the development of new MS treatments, a recent global initiative led by the National MS Society has identified the following three distinct but overlapping cure pathways: (1) stopping the MS disease



(legend on next page)

process, (2) restoring lost functions by reversing damage and symptoms, and (3) ending MS through prevention.⁷ This initiative has also highlighted the need to target the core drivers of disease progression that conventional DMTs fail to counteract, such as chronic central nervous system (CNS) compartmentalized inflammation, failure of remyelination, and ongoing neurodegeneration.⁸

Advanced cell therapies (ACTs), including stem cells, have raised considerable interest, given their potential immunomodulatory and regenerative capabilities.⁹ An extensive body of pre-clinical and early clinical literature is available in support of the capacity of non-hematopoietic stem cell (hNSC) therapies to modulate the host immune responses and facilitate neuroprotection in chronic neurological diseases such as amyotrophic lateral sclerosis (ALS) and Parkinson's disease.^{10,11} Among hNSC therapeutics, those based on somatic brain-specific neural stem/progenitor cells (NSCs) possess key advantages for the treatment of CNS diseases, including their inherent commitment to neural lineage and low tumorigenic risk, due to a general lack of pluripotency and limited proliferation rates.⁹

In vivo studies in rodent and non-human primate models of MS (or MS-like disease) have shown that both syngeneic and xenogeneic (human) NSCs are safe and promote clinicopathological amelioration via multiple mechanisms of action.⁹ Syngeneic NSCs transplanted in rodents with MS-like disease localized and survived in areas of demyelination and axonal loss up to 4 months post-transplantation, only in part differentiating into oligodendrocyte precursor cells (OPCs), astrocytes, and neurons while reducing glial scarring at the lesion sites.^{12,13} The therapeutic properties of human NSCs have also been demonstrated in non-human primate models of MS, where improved functional outcomes and reduced T cell proliferation were observed in animals treated with xenogeneic human NSCs (hNSCs) after intrathecal and intravenous injections.¹⁴ Recent preclinical data suggest that NSCs can target some of the core drivers of MS progression, including the persistent smoldering activation of myeloid cells, when delivered by intracerebroventricular injection (ICVI). NSCs reduce the pro-inflammatory activation of myeloid cells by inducing a metabolic reprogramming of myeloid cells toward oxidative phosphorylation.¹⁵ These data support the delivery of hNSCs via ICVI as a valuable therapeutic option, which would maximize the proportion of cells targeting the CNS and the likelihood of counteracting the smoldering disease processes that drive progressive MS.^{9,16} Despite all this compelling pre-clinical evidence, clinical trials thoroughly testing the feasibility of NSC transplantation in SPMS patients are still needed.

Herein, we report the results of the hNSC-SPMS study, a phase I, open-label, multicenter, dose-escalation clinical trial with a single donor, allogeneic ACT hNSC 03/14b line implanted via ICVI in $n = 15$ patients with active and non-active SPMS.

This is the first and largest clinical trial employing hNSC-based ACTs from a homogeneous cell source in people with SPMS that aims to pave the way for the administration of the same standardized stem cell medicinal product in future clinical trials of efficacy.

RESULTS

The methods for the generation of the clinical-grade hNSC line used in this study all concurred with the implementation of a thoroughly defined cell drug product based on hNSCs,¹⁷ aiming to address some of the issues that are emerging as limiting factors in reliability and reproducibility in the stem cell therapy field.¹⁸

Prior to clinical use, we first assessed the safety, survival, and differentiation of the hNSC 03/14b line following either intra-striatal injection (ISI) or ICVI in athymic Foxn1^{nu} immune-deficient adult mice (Figure 1A). None of the hNSCs-injected mice showed adverse clinical symptoms or developed tumors related to the cellular xenograft up to 6 months after transplantation (Table S1). Necropsy showed no gross alteration in body organs such as the heart, lungs, intestine, liver, kidney, and spleen (not shown). Gross brain pathological analysis showed no evidence of alterations of the cerebral parenchyma, asymmetry of the ventricles, or elements associated with inflammatory or neoplastic processes (Table S1). Transplanted hNSCs were identified by immunohistochemical techniques using an antibody that specifically recognizes the human nucleus (huN) antigen and is not present in host cells. The graft core was clearly identifiable at the delivery site either in the striatum or in the lateral ventricle (Figure 1B). Human NSCs consistently migrated throughout the brain *in vivo*, preferentially along fiber tracts such as the corpus callosum (antero-posterior graft extension: $3,000 \pm 372.5 \mu\text{m}$ for ISI; $4,260 \pm 651.4 \mu\text{m}$ for ICVI). The proportions of viable hNSCs recovered in the brain were $6.7\% \pm 1.7\%$ (ISI) and $5.7\% \pm 1.4\%$ (ICVI) of the total injected (Figure 1C). A small proportion of grafted hNSCs were proliferating and co-expressed Ki67 ($6.1\% \pm 0.2\%$ for ISI; $3.3\% \pm 0.7\%$ for ICVI; not significant) (Figures 1D and 1E), between 11% and 25% expressed the astroglial marker glial fibrillary acidic protein (GFAP, $25.8\% \pm 3.2\%$ for ISI; $11.4\% \pm 1.2\%$ for ICVI; $p < 0.05$) (Figures 1F and 1G), and approximately 9% expressed the neuronal marker β -tubulin III (TUBB3, $9.4\% \pm 3.1\%$ for ISI; $9.2\% \pm 0.2\%$ for ICVI) (Figures 1H and 1I). We also observed clusters of doublecortin⁺ (DCX)-migrating human neuroblasts ($8.5\% \pm 1.1\%$ for ISI; $9.3\% \pm 2.0\%$ for ICVI) (Figures 1J–1H), whereas only a negligible proportion of hNSC xenografts were found to express the OPC marker neural/glia antigen 2 (NG2, not shown). These safety, survival, and differentiation pre-clinical data in immune-deficient Athymic Foxn1^{nu} adult mice are consistent with

Figure 1. Non-clinical parameters of the hNSC 03/14b line after ISI or ICVI in the CNS of healthy immunodeficient mice

(A) Schematic representation of the methodological approach used for the non-clinical characterization of the hNSC 03/14b line.
(B) Confocal representative images of ISI and ICVI hNSC 03/14b line grafts. The insets show a magnification of hNSC nuclei co-labeled with huN (green). Cell nuclei are counter-stained with 4',6-Diamidino-2-Phenylindole (DAPI, blue).
(C–K) (D, F, H, and J) Confocal images and z stacks of the proliferation and differentiation abilities of hNSC 03/14b line grafts *in vivo* upon challenging with the proliferating cell marker Ki67 (red in D), the astroglial marker GFAP (red, in F), and the neuronal markers TUBB3 (red, in H) and DCX (red, in J). Insets and arrowheads identify hNSC-derived huN⁺ cells co-localizing with each marker, which are also shown in the corresponding z stacks and quantified in (C), (E), (G), (I), and (K). Data are represented as mean values \pm SEM. Scale bars: 100 μm in (B), (D), (F), (H), and (J); 40 μm in all z stacks. * $p < 0.05$ (Mann-Whitney test). See also Table S1 and Figure S1.

Table 1. Patient data

Patient #	Dose	Patient ID	Gender	EDSS	Age at diagnosis	Date of conversion to SPMS	Time from conversion (years)	Year of treatment	Age at treatment (years)	Years with MS at treatment	Years with SPMS at treatment
1	5 × 10 ⁶	1151	M	7.5	45	01/01/2010	4	2018	57	24	8
2		1178	M	7	43	01/01/2008	1	2018	54	17	10
3		1181	M	8	34	08/10/2010	12	2018	54	20	8
4	10 × 10 ⁶	1194	M	7.5	24	04/03/2008	4	2018	38	17	10
5		1210	F	7	26	29/04/2010	18	2018	52	26	8
6		1219	F	8	25	01/01/1999	9	2018	53	29	19
7	16 × 10 ⁶	1228	F	7	31	01/01/2010	15	2018	54	24	8
8		1243	F	8	25	01/10/1998	5	2019	51	27	21
9		1249	F	8	34	01/01/2011	6	2019	48	22	8
10	24 × 10 ⁶	1252	F	7.5	38	01/01/2011	6	2019	52	23	8
11		1289	F	8	30	01/06/2016	15	2019	48	18	3
12		1296	M	7	18	01/01/2013	19	2019	43	30	6
13		1316	F	7	33	01/01/2016	20	2019	56	29	3
14		1323	M	8	15	01/01/2004	8	2020	39	26	16
15		1326	F	8	39	N/A	N/A	2020	53	14	N/A

the profile of several other current good manufacturing practice (cGMP)-grade hNSC lines produced by IRCCS “Casa Sollievo della Sofferenza” and characterized according to an established non-clinical evaluation paradigm.¹⁷ The pre-clinical release criteria for ACT hNSC 03/14b line included culturing under cGMP conditions for 10–17 passages *in vitro* (with the last passage being performed 24–96 h before formulation of the final drug product), assessment of clonal efficiency, and differentiation potential after growth factor retrieval *in vitro* (Figure S1). Viability of the released ACT hNSC 03/14b line for transplantation was 79% ± 1.2% (Figure S1).

A total of n = 180 candidates volunteered for hNSC-SPMS transplantation between September 26, 2017 and January 13, 2020. The CONSORT diagram is shown in Figure S2, and the Gantt chart is shown in Table S2. Further details on the study design and inclusion/exclusion criteria are available in the STAR Methods. After screening in one of the two recruiting centers (IRCCS “Casa Sollievo della Sofferenza” Research Hospital [site 1] or “Santa Maria di Terni” Hospital [site 2]), a total of n = 15 active and non-active SPMS patients with an expanded disability status scale (EDSS)¹⁹ ≥ 6.5 and ≤ 8, and evidence of progressive accumulation of disability over the 2 years before recruitment, consented to treatment and were assigned a unique identification number.

Participants, nine females and six males, had a mean age of 50 years (range: 38–57) and were recruited in similar proportions by the two recruiting centers. The mean EDSS was 7.6 (range: 7–8), the mean disease duration was 23 years (range: 14–30), and the mean time from diagnosis to secondary progression was 10 years (range: 1–20). The patients’ detailed demographic and clinical characteristics are reported in Table 1.

A 3-month run-in period was carried out to establish the clinical and radiological baseline features of each patient before treatment (Table S2). All patients were then randomly enrolled into four treatment cohorts receiving four dosages (5, 10, 16, and 24 million [M] cells) of the single donor, homogeneous, allo-

genic ACT hNSC 03/14b line¹⁷ via ICVI, according to a standard dose-escalation method that followed a modified Fibonacci sequence (100%, 60%, and 50% dose increments; Figure 2; Table 1).

The primary objective of the study was to assess the feasibility, safety, and tolerability of treatment by evaluating the mortality and the number and type of adverse events (AEs) leading to the maximum tolerated dose. The secondary objective was to evaluate the potential therapeutic effects of hNSCs by monitoring disease progression during the 12-month follow-up period. See also Table S2 and STAR Methods.

At the time of treatment, patients were admitted to the Neurosurgery Unit of site 2 to undergo a single ICVI of the ACT hNSC 03/14b line. Thin-slice cranial computed tomography (CT) or magnetic resonance imaging (MRI) scans were performed to evaluate the ventricular system and plan the procedure. A frameless stereotactic image guidance AxiEM system (Stealth Station AxiEM Electromagnetic Tracking System, Medtronic Navigation, Louisville, CO, USA) was used to perform the ventricular cannulation (Figure 3). The correct catheter placement was verified based on the egress of cerebrospinal fluid (CSF), and a Rickham reservoir was then connected to it. After batch release (Figure S1), ACT hNSCs 03/14b line were counted and suspended in Hank’s balanced salt solution (HBSS) at a concentration of 50,000 cells/μL and maintained at 4°C ± 2°C for up to 1.5 h prior to implantation. In a small number of cases (n = 3), we also recovered a small number of cells from the needle post-surgery, which were cultured and expanded for additional five passages showing no differences in either growth abilities or differentiation potential compared with the injected drug product (Figure S3), further supporting the stability of the ACT hNSC 03/14b line.

All participants underwent a CT scan within 24 h from surgery to evaluate post-surgery complications and received oral methylprednisolone once (125 mg, 2 h pre-intervention), intravenous cefazolin twice (1 g, pre- and post-hNSC injection), and daily oral prednisone with a 28-day tapering (each week from 60,

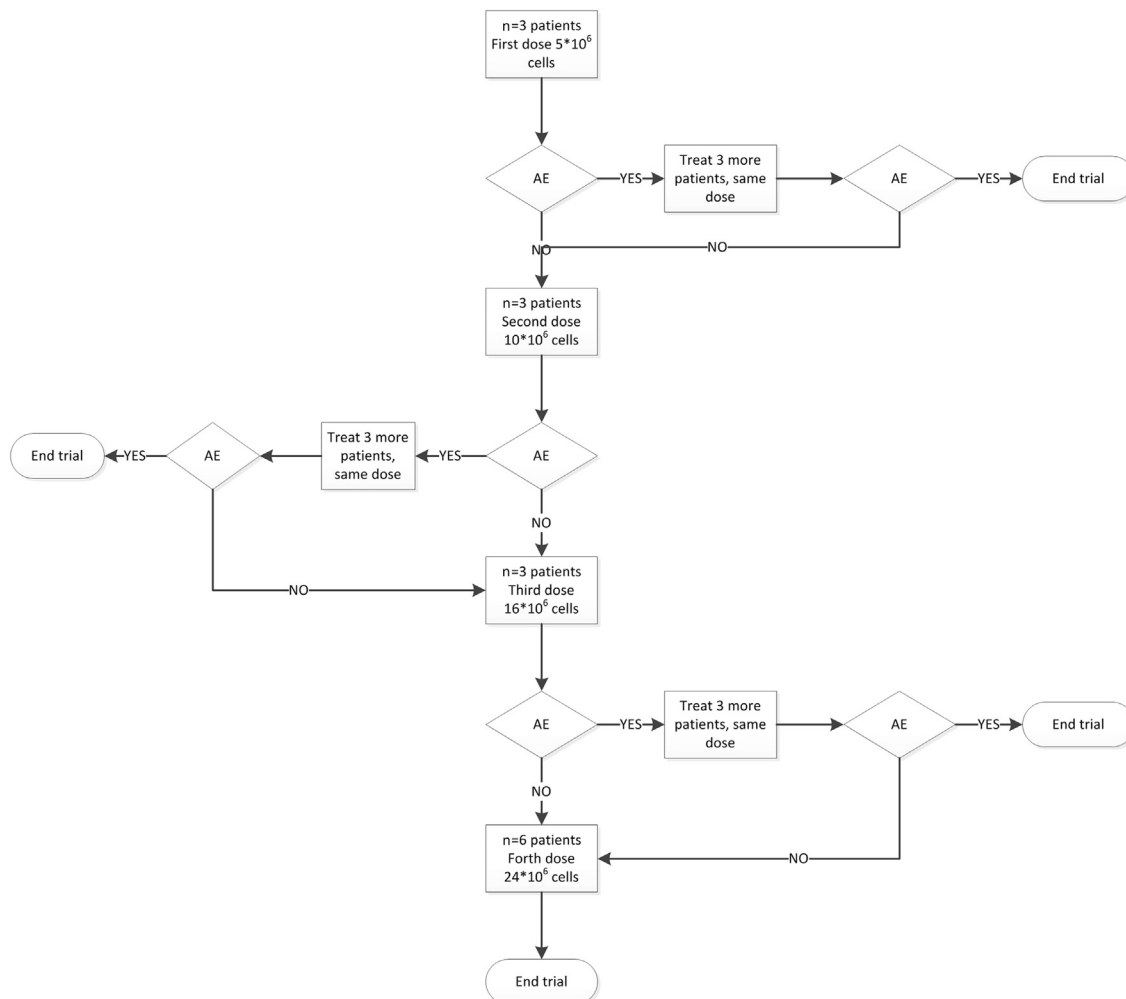


Figure 2. Fibonacci ACT dose-escalation scheme

To find the recommended phase II dose, we used “standard” phase I design with a “Fibonacci” dose escalation scheme of 100%, 67%, and 50%. Thus, the second dose level is 100% greater than the first, the third is 67% greater than the second, and so forth (5, 10, 16, and 24 million cells). See also [STAR Methods](#). See also [Figure S2](#) and [Tables 1](#) and [2](#).

40, 20, to 10 mg/day). Participants also received oral tacrolimus (0.05 mg/kg twice a day) 12 h after the intervention and every 12 h for the first 6 months. Tacrolimus was titrated to maintain blood levels within a 5–10 ng/mL range. Further details on the transplantation procedure are available in the [STAR Methods](#).

Study participants were followed for 12 months post-ICVI with monthly visits ([Table S2](#)). The vital signs of the participants (blood pressure and temperature) were within the normal range, and urine tests did not show significant clinical abnormalities (not shown). Among laboratory exams, the only clinically significant variation was in the number of white blood cells that ranged from a mean of $7.4 \times 10^9/L$ at run-in-END period to a mean of $8.3 \times 10^9/L$ at the 12-month follow-up (not shown).

Evaluations of health status and mortality were based on the occurrence of serious co-morbidities, changes in general health, and the number of deaths due to the treatment (or to the procedure itself). All AEs were recorded and evaluated by the attending neurologists for any potential relationship with the ICVI of the ACT

hNSC 03/14b line ([Table 2](#)). Disease progression was monitored via EDSS, multiple sclerosis functional composite (MFSC, [Table S3](#)), annualized relapse rate, and time to confirmed relapse, whereas cognitive function was assessed by Rao’s brief repeatable battery (BRB, not shown). The last patient visit (12 months of follow-up) was in April 2021 ([Table S2](#)).

Neither deaths nor serious AEs occurred in any patient after treatment during the 12-month follow-up period ([Table 2](#)). The immunosuppressive treatment was well tolerated and completed by all patients without serious AEs. One patient (1/15; 6.6%) developed a steroid-induced psychosis at 1-month post-hNSC injection but recovered completely within 1 month with the administration of valproate, lorazepam, olanzapine, and psychotherapy. Another patient (1/15; 6.6%) developed a tremor during tacrolimus treatment, which disappeared following dose-adjustment. Minor infections were detected in three patients (3/15; 20%; 1 upper respiratory tract, 2 urinary tract). All other reported AEs were related to non-study concomitant therapy or other

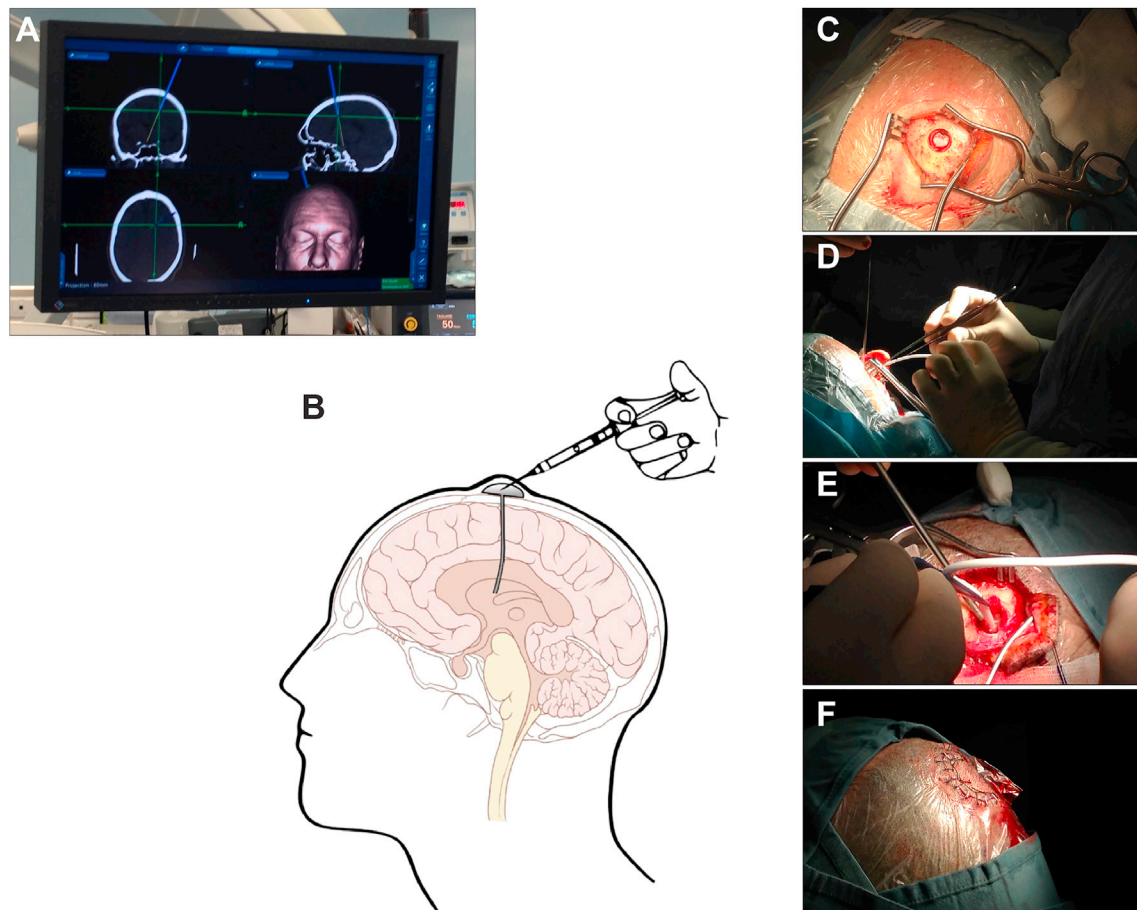


Figure 3. hNSC ICVI procedure

(A) Thin-slice cranial CT or MRI scans allow the evaluation of the ventricular system.

(B–F) Frameless stereotactic image guidance AxiEM system used to perform the ventricular cannulation. Correct catheter placement is verified based on the egress of CSF, and a Rickham reservoir is then connected to it. (B) was released to the public domain by its author, Patrick L. Lynch. You may find the image at https://commons.wikimedia.org/wiki/File:Ommaya_01.png#file. See also [Figures S1](#) and [S3](#).

medical conditions unrelated to the experimental protocol ([Table 2](#)).

No changes in functional disability and clinical progression of the disease were recorded in the 12-month follow-up period ([Table S3](#)). Two patients (2/15; 13.3%) had a change in a single functional score (FS) of >1 point in the pyramidal area: one patient's score decreased from 4.5 to 3.0, and the other one increased from 0.0 to 2.0. None of the patients reported symptoms indicative of a relapse, and cognitive function did not significantly worsen during the study.

The potential effects of the treatment were explored by testing for accepted fluid biomarkers of astrocytosis, inflammation, and neuronal loss at run-in-START and run-in-END, and then at +1, +6, and +12 months post-treatment (in the CSF) and at 1, 3, 6, 9, and 12 months post-treatment (in the serum) (see [STAR Methods](#)). Most of the molecules evaluated in patients' serum and CSF showed no significant changes with disease course or treatment, i.e., C-C motif chemokine ligand 2 (CCL2), C-C motif chemokine ligand 3 (CCL3), fractalkine, vascular endothelial growth factor-A (VEGF-A), Chitinase 3 Like 1 (CHI3L1), Osteopontin (OPN), interleukin (IL)-17a, IL-8, tumor ne-

crosis factor alpha (TNF- α), and IL-2 ([Tables S4A–S4D](#)). GFAP concentrations in the CSF and serum remained stable throughout the trial for all the hNSC dose groups ([Tables S4E](#) and [S4F](#)). Neurofilament light-chain (NfL) concentrations showed a statistically significant increase at 1 month post-surgery both in CSF (overall concentration from 791.44 to 1,630.5 pg/mL) and serum (overall concentration from 13.70 to 49.19 pg/mL), followed by a gradual return to pre-treatment values (overall concentration in CSF 1,050.1 pg/mL at 6 months and in serum 15.06 pg/mL at 9 months) across the four dose groups ([Figure S4](#); see also [Tables S4E](#) and [S4F](#)).

At the same time points used for the fluid biomarkers, we also performed untargeted metabolomic and lipidomics analyses of the CSF and serum ([Figure 4A](#); details in [STAR Methods](#)). Data at run-in-START showed no clear differences in the CSF metabolomes and lipidomes in the patient population, as determined by unsupervised principal component analysis ([Figure S5](#)). On the other hand, baseline differences in serum lipidomes were observed ([Figure S5](#)), although these differences were maintained across all time points and did not change as a function of hNSC doses ([Figure 4C](#)).

Table 2. Adverse events

Patient #	Patient ID	hNSC 04/13b dose	Description of event	Expected	Severity	Relationship to study therapy	Action taken	If other, please specify	New treatment/therapy given/taken	Outcome (at the end of the study)
#1	1151	5 × 10 ⁶	tremor	yes	mild	unrelated	tacrolimus dose changed	N/A	no	recovered
			flu like syndrome	no	mild	unrelated	none	N/A	yes	recovered
			respiratory failure	yes	mild	unrelated	concomitant therapy changed	N/A	yes	recovered
			cataract (left eye; surgical procedure)	no	mild	unrelated	none	N/A	no	recovered
			upper respiratory infection	no	mild	unrelated	concomitant therapy changed	N/A	yes	recovered
#2	1178	5 × 10 ⁶	hyperglycaemia	yes	moderate	unrelated	concomitant therapy changed	N/A	no	recovered
			urinary retention	yes	moderate	unrelated	other, specify	catheterization	yes	recovering (improving)
			back pain	no	mild	unrelated	other, specify	new therapy given	yes	recovered
#3	1181	5 × 10 ⁶	none	N/A	N/A	N/A	N/A	N/A	N/A	
#4	1194	10 × 10 ⁶	seizure	yes	mild	unrelated	other, specify	diazepam, levetiracetam	yes	recovered
#5	1210	10 × 10 ⁶	none	N/A	N/A	N/A	N/A	N/A	N/A	N/A
#6	1219	10 × 10 ⁶	none	N/A	N/A	N/A	N/A	N/A	N/A	N/A
#7	1228	16 × 10 ⁶	psychosis	no	moderate	unrelated	concomitant therapy changed	N/A	yes	recovered
#8	1243	16 × 10 ⁶	none	N/A	N/A	N/A	N/A	N/A	N/A	N/A
#9	1249	16 × 10 ⁶	leukoencephalopathy	no	mild	unrelated	other, specify	MRI evaluations	no	recovering (improving)
			urinary tract infection	no	mild	unrelated	other, specify	drugs administration	yes	recovered
#10	1252	24 × 10 ⁶	none	N/A	N/A	N/A	N/A	N/A	N/A	N/A
#11	1289	24 × 10 ⁶	none	N/A	N/A	N/A	N/A	N/A	N/A	N/A
#12	1296	24 × 10 ⁶	depression	no	moderate	unrelated	none	N/A	no	unknown
#13	1316	24 × 10 ⁶	none	N/A	N/A	N/A	N/A	N/A	N/A	N/A
#14	1323	24 × 10 ⁶	urinary tract infection	no	mild	unrelated	other, specify	antibiotics administration	yes	nNot recovered
#15	1326	24 × 10 ⁶	none	N/A	N/A	N/A	N/A	N/A	N/A	N/A

N/A, not applicable.

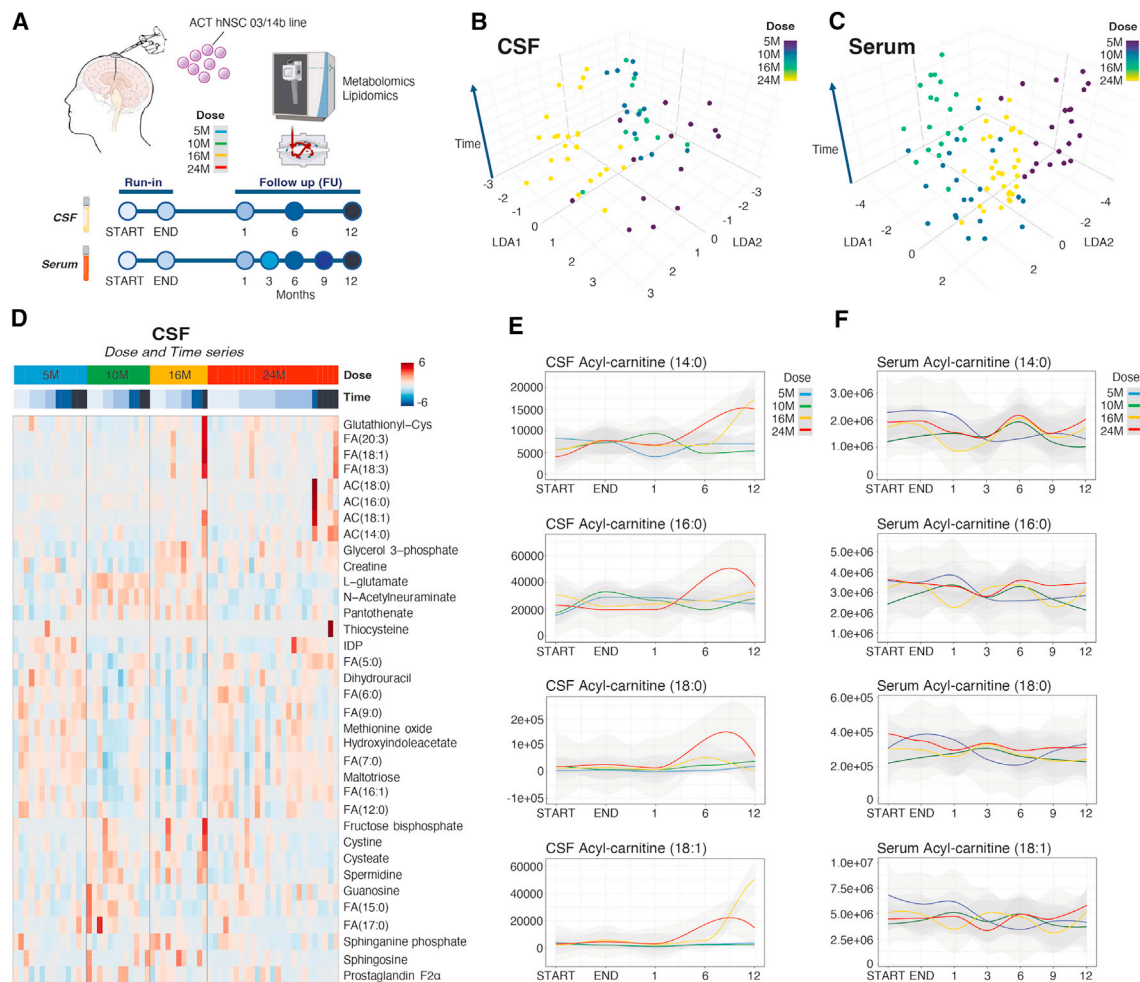


Figure 4. Longitudinal metabolomics and lipidomics analyses of CSF and serum

(A) Experimental design.

(B and C) Linear discriminant analyses (LDAs) identify an effect of ACT hNSC 03/14b line dose and time (z axis) on the metabolic phenotypes with a clear dose-dependent gradient in the CSF (B), but not in the serum (C).

(D) Two-way ANOVA (time series and dose) identified significant metabolic and lipid changes in CSF.

(E and F) Line plots showing the time and dose-dependent response of long-chain AC (14:0, 16:0, 18:0, and 18:1) in the CSF (E) and serum (F) of treated patients. See also Figure S5.

Therefore, we next performed a hierarchical clustering of the most significant CSF metabolites and lipids as a function of hNSC dose and time over the course of the clinical trial. This analysis showed temporal and dose-dependent changes in CSF levels of markers of fatty acid (FA) oxidation and catabolism, including acyl-carnitines (AC), free FA, odd-chain FAs, coenzyme A (CoA) precursors (pantothenate), and glycerol 3-phosphate (Figure 4D). When CSF metabolomics and lipidomics results were correlated to clinical covariates, network analyses confirmed FA (very long-chain and poly or highly unsaturated ones of the 18C and 20C series) and AC as main nodes with a high degree of betweenness centrality, and the levels of these metabolites were significantly correlated to hNSC dose and subject (Figure S5C). Importantly, we found that patients receiving the highest hNSC doses (both 16 M and 24 M) had the highest increase in CSF levels of long-chain AC (14:0, 16:0, 18:0, and 18:1) at the end of the follow-up period (Figure 4E). These dose- and time-dependent effects

were not evident when the same AC species were analyzed in the serum (Figure 4F).

Brain MRIs were performed at run-in-START and run-in-END, as well as during the 12-month follow-up period, to monitor structural changes related to intervention, disease activity, and unexpected findings (see STAR Methods). MRIs were acquired at the two recruiting centers, whereas image analysis was performed at the Multiple Sclerosis Center of the Neurocenter of Southern Switzerland (site 3) aiming to detect (1) differences in lesion load between serial imaging and (2) variations of parenchymal brain volume changes (PBVCs) (Table S5). Data from the run-in period showed that ~50% of the enrolled patients had at least one new or one enlarging T2-visible lesion, whereas 43% of the patients had at least one lesion with contrast enhancement (Table S6). Compared with the run-in, during the 12 months following transplantation, 9 of the 15 patients (60%) presented a greater

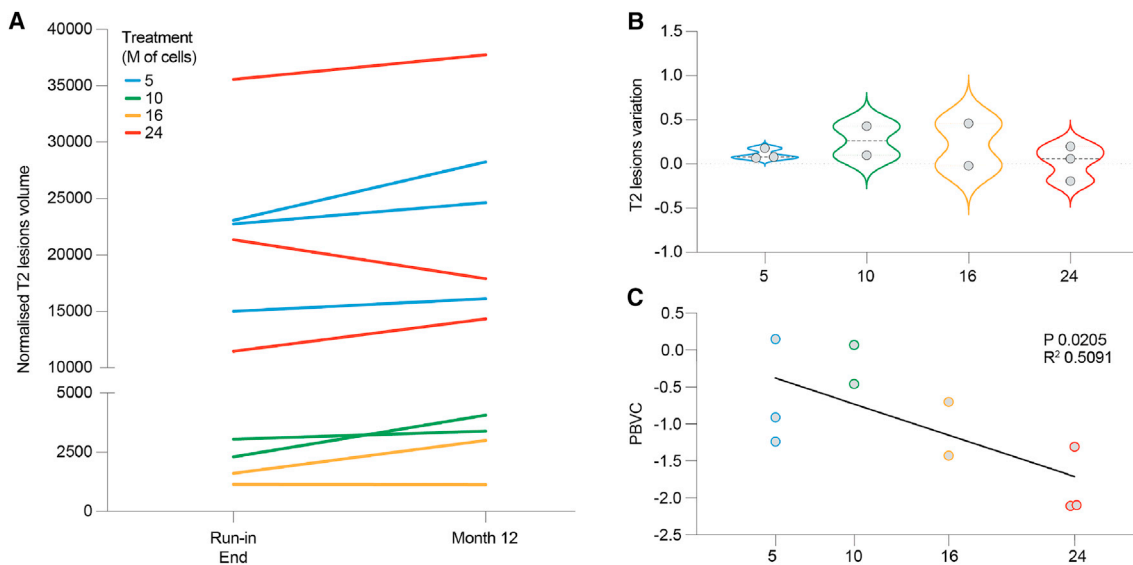


Figure 5. MRI results

(A) Normalized volume of T2 lesions between the run-in-END and month 12 according to the four different doses of ACT hNSC 03/14b: 5, 10, 16, and 24 million cells. Each line is an individual patient.
 (B) Variation of T2 lesions between the run-in-END and month 12 according to the four different doses of ACT hNSC 03/14b as in (A). Each dot is an individual patient.
 (C) Spearman's analysis of the correlation between the dose of injected ACT hNSC 03/14b and PBVC. The straight line depicts the linear regression. $p = 0.0205$; $R^2 = 0.5091$. See also [Tables S6–S8](#).

number of new/enlarging T2-visible lesions ([Table S7](#)), and 6 of the 15 patients (40%) demonstrated a greater number of contrast-enhancing lesions ([Table S8](#)). However, 5 of the 15 (33.3%) patients also showed the absence of new and/or enlarging T2-visible lesions, whereas 3 of the 15 (20%) developed the same or a smaller number of contrasts enhancing lesions during the 12-month post-ICVI of the ACT hNSC 03/14b line ([Table S8](#)). None of these MRI findings did correlate with the dose of injected hNSCs.

After treatment, we identified and categorized the following new-onset parenchymal changes: type 1 changes (likely surgery related) ([Figure S6](#)), type 2 changes (likely MS disease-related, according to the 2017 revisions of the McDonald criteria)²⁰ including T2-visible and contrast-enhancing lesions, and type 3 changes (other/undetermined), based on the literature knowledge^{21,22} and the readers' expertise ([Figure S7](#)). No unexpected/acute findings were detected in any examination, apart from MS-related disease activity. Specifically, we found that during the 12-month follow-up period, 10 of the 15 (66%) patients had at least one new or one enlarging T2-visible lesion (64 new-onset, including 3 enlarging T2-visible lesions, were detected with an average of 6.4 and 0.3 of new and enlarging T2 lesions per patient, respectively) ([Table S7](#)). When we compared the annualized pre- vs. post-surgery rate of new or enlarging T2-visible lesions (3.30, 95% CI: 1.86–5.83 vs. 4.72, 95% CI: 2.32–9.61), we found no statistically significant difference ($p = 0.26$). A total of 8 of the 15 (53%) patients had at least one lesion with contrast enhancement during the 12-month follow-up period ([Table S8](#)), and we found that the annualized pre-surgery lesion rate of contrast enhancement lesions was not statistically different ($p = 0.98$)

from post-surgery values (2.86, 95% CI: 1.51–5.40 vs. 2.83, 95% CI: 0.92–8.73). A subgroup of $n = 10$ patients who had both baseline (run-in-END) and final follow-up (month 12) imaging were further assessed for T2 lesion load and changes in PBVCs. However, we found no significant differences in T2 lesion loads ([Figures 5A](#) and [5B](#)). Spearman's analysis revealed a significant inverse correlation between the dose of injected hNSCs and PBVCs (Spearman's $\rho = -0.7$, $p = 0.0205$) ([Figure 5C](#)).

DISCUSSION

The hNSC-SPMS study shows that the ICVI of the single donor, allogeneic ACT hNSC 03/14b line in people with active and non-active SPMS patients is safe and well tolerated and so is the proposed immunosuppressive treatment. No deaths, adverse reactions (ARs), or withdrawals were registered. All AEs were reversible and related to concomitant therapies (steroids, tacrolimus). Only one subject developed a mild partial motor seizure at month 6, which was treated with diazepam and levetiracetam. This AE was possibly related to MS, as described.^{23,24} However, we cannot exclude the possibility of it being related to the ACT delivery procedure. No other symptoms or disease developed during the follow-up, and the quality of life (QOL) evaluation did not change, showing a general good tolerance for the whole procedure.

Results for laboratory tests also did not significantly change during the follow-up. John Cunningham Virus (JCV) testing in the CSF remained negative. Also, despite an initial fluctuation of the levels of CSF and serum NfL after surgery, this marker later returned to baseline values. Metabolomics and lipidomics

analyses of matched CSF and serum samples revealed a time- and dose-dependent response with an increase of FA and AC in the CSF at follow-up. Indeed, we found an association between hNSC dose and odd-chain saturated FA in the CSF that—in the absence of noticeable changes in the patients' dietary habits—may result from a process of α -oxidation, involving the activation, then hydroxylation of the α -carbon of long-chain FA, followed by the removal of the terminal carboxyl group.²⁵ Levels of long-chain AC were also found to have a time- and dose-dependent increase in the CSF of treated MS patients but not in the serum, which may suggest an increased availability of substrates for β -oxidation in the CNS.²⁶ Although previous studies found that MS patients have generally low levels of circulating AC in the blood vs. healthy controls,^{27,28} the link between the ICVI of hNSC and changes in the CSF AC levels needs to be further explored. In keeping with Genchi et al., we also observed an alteration of glycerol 3-phosphate in CSF upon treatment, an observation that can be explained by altered complex lipid synthesis or catabolism.²⁹ In addition, a group of carboxylic acids—including lactate, citrate, malate, and oxaloacetate—clustered together and correlated with acyl-carnitine metabolism, suggesting a potential role of CSF AC metabolism as a therapeutic target for immunomodulatory therapies in MS.³⁰

Clinical measures of disability (EDSS and MSFC) and cognitive outcomes did not change significantly throughout the follow-up. Most importantly, none of the patients showed clinical relapses. Overall, this points to a substantial stability of the disease, without signs of progression, although changes in some of these parameters could be hard to evince at these high levels of disability.

The MRI inflammatory activity, assessed by an annualized rate of new or enlarging T2-visible lesions and lesions with contrast enhancement, was not affected by the treatment. Noteworthy, our analysis evidenced lesion activity occurring throughout the 12-month post-surgery period. However, it is difficult to identify a causal effect of the hNSCs transplantation on this feature, as the same was also observed in the run-in, prior to treatment. Moreover, literature exists that the amount of MRI activity in people with SPMS might depend on the frequency of scanning^{29,31}; in particular, Tubridy et al. reported a rate of lesion activity similar to our study on SPMS patients who underwent a monthly brain MRI schedule for 4 months.

In the subgroup of patients in whom we assessed the PBVCs, a larger dose of injected hNSCs correlated with smaller PBVCs. A similar observation was reported by Genchi et al. in their recent neural stem cell transplantation in multiple sclerosis patients (STEMs) study,²⁹ in which this was interpreted as a reduction in brain inflammation. Caution is advised in this respect, and neither our study nor STEMs discriminate against the potential mechanism that may underlie this phenomenon. Nonetheless, it is also possible to speculate that hNSCs might have dampened inflammation, thereby leading to edema resolution and pseudoatrophy. This is an expected occurrence seen in patients with MS treated with highly effective immunomodulatory DMTs³² and might explain our observations. However, given the study's uncontrolled design and small sample size and the lack of apparent benefit specifically on MRI lesion activity, it is plausible not to exclude a potential deleterious effect of the treatment or the role of additional factors on neuroinflammation such as the immunosuppression. In this view, extended longitudinal investigations that include

MRI-based assessment of myelin and water content are needed to address this key aspect of brain damage and repair.³³

Compared with previous trials, the hNSC-SPMS study also brings about some key novelties. hNSC-SPMS focused on a homogeneous population of 15 human subjects with SPMS. For the first time, we also favored ICVI of cells so that the hNSCs were administered near key diseased brain regions (e.g., periventricular white matter and choroid plexus), where they might also penetrate the surrounding parenchyma, as shown by extensive feasibility, safety, and efficacy pre-clinical data collected in both rodent and non-human primate models of MS-like disease over the last 15+ years.^{12–14}

More substantial differences exist between hNSC-SPMS and previous trials when taking into consideration the most important element in these ACT studies, namely the transplanted hNSCs, which is the cell drug itself. Regarding the latter, a series of key scientific and methodological issues that are a major cause for the inconsistent outcomes observed in many clinical, ACT endeavors need to be examined. Intra- and inter-trial erratic results in ACT are chiefly due to the variable compositions and properties of the cell drugs used in otherwise similar studies,¹⁸ which often arises from their loose, faulty, or incomplete characterization through manufacturing. This issue becomes crucial when working with progenitor cells expanded extensively in culture, as in the case at hand. By their inherent properties, the *ex vivo* propagation of human neural precursors leads to mixed cultures of hNSCs and additional, more mature, functionally heterogeneous, neural progenitor populations.³⁴ The relative proportions of these populations appreciably fluctuate over time and serial passaging, even within the same culture. Thus, ACT trials aiming at delivering hNSC, rather than an unwanted, undetermined mixture of brain cells, must specifically monitor the size of the hNSC pool in their cell drug.¹⁸ This is accomplished by the routine, detailed monitoring of a defining set of hNSC functional properties (EudraLex Good Manufacturing Practice Specific to Advanced Therapy Medicinal Products; <https://health.ec.europa.eu>). The hNSC-SPMS study specifically adopted this approach by the routine certification of an established panel of hNSC-specific functional tests at each step throughout cell propagation, up to transplantation, to warrant the implantation of a pre-determined, stable content of hNSCs. To refine this process, 48–96 h prior to the intervention, a final selection step eliminated the more mature elements in the culture and retained exclusively the highly immature, clonogenic cells (see also *STAR Methods*). These were transplanted within 20 min from harvesting, with a viability index averaging ~80%. Thanks to the sustained propagation capacity of the technique used in hNSC-SPMS, not only the patients in this study but also all the participants in similar future trials will be transplanted with the very same hNSC drug, which warrants stable and predictable composition and properties. This makes it so that the availability of hNSCs for future clinical trials will no longer be a limiting factor and that future clinical studies can be carried out by adopting a centralized production center that will distribute the very same cell drug to multiple clinical sites. We feel that this approach promises to greatly reduce the issue of variability in future hNSC clinical transplantation.

The hNSCs in this study were derived from miscarriages, with tissue procurement procedures identical to those for organ

donation. Thus, an additional advantage coming from our study may be that of making available a clinical-grade, continuous cell source for future ACT clinical trials that is less prone to those ethical criticisms that are often associated with the procurement of human fetal tissue.

Limitations of the study

Inevitably, there are limitations to the import of our study, which, in good part, pertain to it being an early-stage, first-in-men, phase I study, compounded by the fact that the targeted organ is the brain of people with late-stage SPMS; however, its likely poor accessibility and inherent structural fragility for this disease stage, hence, limit the potential for the window of opportunity addressed by the hNSC-SPMS study. Additional elements in this consideration emerge from the novel, peculiar, and experimental nature of the ACT drug at hand.

Being a phase 1 human study, hNSC-SPMS inevitably falls short in both statistical power, the lack of a placebo control group, and a relatively short follow-up, thereby limiting the breadth of some of the conclusions regarding efficacy. Although the design of hNSC-SPMS attempted to reduce the impact of the latter factor by including a 3-month run-in prior to patient enrolment and randomization into treatment, this whole unique situation did prevent unequivocally ruling out the possibility that some of the encouraging outcomes collected (e.g., the inverse correlation between the amount of injected hNSCs and PBVC at the MRI) may be attributed solely to the multimodal biological effects of the injected ACT hNSC 03/14b line.

Our attempt at determining the metabolic impact of the intervention, given the role of metabolic regulation in immunometabolism in the onset and progression of MS,^{9,16} was also limited by the very nature of the study design, where each patient's initial conditions at enrolment represent their own paired controls and the metabolic profiles of untreated control patients were lacking. However, our metabolomics and lipidomics analyses confirmed and expanded upon the literature by providing longitudinal analyses of CSF as a function of intervention, with dose-dependent responses to live hNSCs, correlated with functional outcomes.

Last, the nature of the intervention and the allogeneic (hence potentially immunogenic) origin of the ACT hNSC 03/14b line did impose the concomitant, yet medium-term, administration of a combination of systemic anti-inflammatory and immunosuppressant medications, whose effects may somewhat impact the interpretation of the results.

Although our extensive animal work points to the ability of both syngeneic and xenogeneic NSC grafts to dampen inflammation and provide neuroprotection at different levels and at the same time to progress toward cell differentiation, integration, and replacement *in vivo*; however, the mechanism(s) of action of this novel ACT drug remains undetermined, given the impossibility to document donor cell survival, integration, and fate following transplantation in human subjects.

STAR★METHODS

Detailed methods are provided in the online version of this paper and include the following:

- **KEY RESOURCES TABLE**
- **RESOURCE AVAILABILITY**
 - Lead contact
 - Materials availability
 - Data and code availability
- **EXPERIMENTAL MODEL AND STUDY PARTICIPANT DETAILS**
 - 03/14b human Neural Stem Line
 - Animals safety study
 - Clinical trial design and patient selection
- **METHOD DETAILS**
 - hNSC culture and characterization
 - Animal studies: surgery, behavior, histology
 - Study design
 - Inclusion and exclusion criteria
 - hNSCs transplantation in people with SPMS
 - Outcome measures
 - Clinical and laboratory evaluation
 - Mass spectrometry-based metabolomics and lipidomics analysis
 - Magnetic resonance imaging (MRI)
 - Data management and study monitoring
- **QUANTIFICATION AND STATISTICAL ANALYSIS**
- **ADDITIONAL RESOURCES**

SUPPLEMENTAL INFORMATION

Supplemental information can be found online at <https://doi.org/10.1016/j.stem.2023.11.001>.

ACKNOWLEDGMENTS

The authors thank J. Chataway, P. Chinnery, A. Coles, F. Dazzi, V. Fossati, D. Franciotta, R. Magliozzi, and G. Pluchino for critically discussing the article. The authors acknowledge the contribution of past and present members of the Pluchino and Vescovi laboratories who have contributed to (or inspired) this study. Writing, proofreading, and submission assistance were provided by Maria Carolina Rojido and Laura C. Collada Ali, respectively. This work has been partially funded by the Italian Minister of Health, Ricerca Corrente 2022–2024. Special thanks go to the "ASSICURAZIONI GENERALI" group, whose continued sponsorship was fundamental to the success of this research. The graphical abstract was generated with the support of Molecular House (<https://molecular.house>). Support for writing, proofreading, and submission assistance was funded by IRCCS "Casa Sollievo della Sofferenza" Research Hospital, Italy, and Revert Onlus. L.P.-J. was supported by a Wellcome Trust Clinical Research Career Development Fellowship G105713. The University of Colorado School of Medicine Metabolomics Core is supported in part by the University of Colorado Cancer Center award from the National Cancer Institute P30CA046934. The sponsors of this study had no role in the collection, analysis, and interpretation of the data nor in the writing of the report and in the decision to submit the paper for publication.

AUTHOR CONTRIBUTIONS

M.A.L. and M.G. prepared the manuscript with contributions from D.C.P., C.G., E.P., A.D'A., L.P.-J., S.P., and A.L.V. C.C. and A.C. performed surgical procedures. All authors contributed to study design, sample or data collection, and/or data analysis or interpretation. All authors approved the final version of the manuscript.

DECLARATION OF INTERESTS

S.P. is founder, CSO, and shareholder (>5%) of CITC Ltd. and Chair of the Scientific Advisory Board at ReNeuron plc.

INCLUSION AND DIVERSITY

We support inclusive, diverse, and equitable conduct of research.

Received: June 23, 2023

Revised: September 11, 2023

Accepted: November 1, 2023

Published: November 27, 2023

REFERENCES

1. Stenager, E. (2019). A global perspective on the burden of multiple sclerosis. *Lancet Neurol.* 18, 227–228. [https://doi.org/10.1016/S1474-4422\(18\)30498-8](https://doi.org/10.1016/S1474-4422(18)30498-8).
2. Derfuss, T., Mehling, M., Papadopoulou, A., Bar-Or, A., Cohen, J.A., and Kappos, L. (2020). Advances in oral immunomodulating therapies in relapsing multiple sclerosis. *Lancet Neurol.* 19, 336–347. [https://doi.org/10.1016/S1474-4422\(19\)30391-6](https://doi.org/10.1016/S1474-4422(19)30391-6).
3. Scalfari, A., Neuhaus, A., Daumer, M., Muraro, P.A., and Ebers, G.C. (2014). Onset of secondary progressive phase and long-term evolution of multiple sclerosis. *J. Neurol. Neurosurg. Psychiatry* 85, 67–75. <https://doi.org/10.1136/jnnp-2012-304333>.
4. Brown, J.W.L., Coles, A., Horakova, D., Havrdova, E., Izquierdo, G., Prat, A., Girard, M., Duquette, P., Trojano, M., Lugaresi, A., et al. (2019). Association of initial disease-modifying therapy with later conversion to secondary progressive multiple sclerosis. *JAMA* 321, 175–187. <https://doi.org/10.1001/jama.2018.20588>.
5. Kolind, S., Gaetano, L., Assemal, H.E., Bernasconi, C., Bonati, U., Elliott, C., Hagenbuch, N., Magon, S., Arnold, D.L., and Traboulsee, A. (2023). Ocrelizumab-treated patients with relapsing multiple sclerosis show volume loss rates similar to healthy aging. *Mult. Scler.* 29, 741–747. <https://doi.org/10.1177/13524585231162586>.
6. Confavreux, C., and Vukusic, S. (2014). The clinical course of multiple sclerosis. *Handb. Clin. Neurol.* 122, 343–369. <https://doi.org/10.1016/B978-0-444-52001-2.00014-5>.
7. Bebo, B.F., Jr., Allegretta, M., Landsman, D., Zackowski, K.M., Brabazon, F., Kostich, W.A., Coetzee, T., Ng, A.V., Marrie, R.A., Monk, K.R., et al. (2022). Pathways to cures for multiple sclerosis: A research roadmap. *Mult. Scler.* 28, 331–345. <https://doi.org/10.1177/13524585221075990>.
8. Reich, D.S., Lucchinetti, C.F., and Calabresi, P.A. (2018). Multiple sclerosis. *N. Engl. J. Med.* 378, 169–180. <https://doi.org/10.1056/NEJMr1401483>.
9. Pluchino, S., Smith, J.A., and Peruzzotti-Jametti, L. (2020). Promises and limitations of neural stem cell therapies for progressive multiple sclerosis. *Trends Mol. Med.* 26, 898–912. <https://doi.org/10.1016/j.molmed.2020.04.005>.
10. Mazzini, L., Gelati, M., Profico, D.C., Sgaravizzi, G., Progetti Pensi, M., Muzi, G., Ricciolini, C., Rota Nodari, L., Carletti, S., Giorgi, C., et al. (2015). Human neural stem cell transplantation in ALS: initial results from a phase I trial. *J. Transl. Med.* 13, 17. <https://doi.org/10.1186/s12967-014-0371-2>.
11. Alessandrini, M., Preynat-Seaue, O., De Bruin, K., and Pepper, M.S. (2019). Stem cell therapy for neurological disorders. *S. Afr. Med. J.* 109, 70–77. <https://doi.org/10.7196/SAMJ.2019.v109i8b.14009>.
12. Pluchino, S., Quattrini, A., Brambilla, E., Gritti, A., Salani, G., Dina, G., Galli, R., Del Carro, U., Amadio, S., Bergami, A., et al. (2003). Injection of adult neurospheres induces recovery in a chronic model of multiple sclerosis. *Nature* 422, 688–694. <https://doi.org/10.1038/nature01552>.
13. Pluchino, S., Zanotti, L., Rossi, B., Brambilla, E., Ottoboni, L., Salani, G., Martinello, M., Cattalini, A., Bergami, A., Furlan, R., et al. (2005). Neurosphere-derived multipotent precursors promote neuroprotection by an immunomodulatory mechanism. *Nature* 436, 266–271. <https://doi.org/10.1038/nature03889>.
14. Pluchino, S., Gritti, A., Blezer, E., Amadio, S., Brambilla, E., Borsellino, G., Cossetti, C., Del Carro, U., Comi, G., t Hart, B., et al. (2009). Human neural stem cells ameliorate autoimmune encephalomyelitis in non-human primates. *Ann. Neurol.* 66, 343–354. <https://doi.org/10.1002/ana.21745>.
15. Peruzzotti-Jametti, L., Bernstock, J.D., Vicario, N., Costa, A.S.H., Kwok, C.K., Leonardi, T., Booty, L.M., Bicci, I., Balzarotti, B., Volpe, G., et al. (2018). Macrophage-derived extracellular succinate licenses neural stem cells to suppress chronic neuroinflammation. *Cell Stem Cell* 22, 355–368.e313. <https://doi.org/10.1016/j.stem.2018.01.020>.
16. Peruzzotti-Jametti, L., Willis, C.M., Hamel, R., Krzak, G., and Pluchino, S. (2021). Metabolic control of smoldering neuroinflammation. *Front. Immunol.* 12, 705920. <https://doi.org/10.3389/fimmu.2021.705920>.
17. Profico, D.C., Gelati, M., Ferrari, D., Sgaravizzi, G., Ricciolini, C., Progetti Pensi, M., Muzi, G., Cajola, L., Copetti, M., Ciusani, E., et al. (2022). Human neural stem cell-based drug product: clinical and nonclinical characterization. *Int. J. Mol. Sci.* 23, 13425. <https://doi.org/10.3390/ijms232113425>.
18. Turner, L. (2021). ISSCR's Guidelines for Stem Cell Research and Clinical Translation: supporting development of safe and efficacious stem cell-based interventions. *Stem Cell Rep.* 16, 1394–1397. <https://doi.org/10.1016/j.stemcr.2021.05.011>.
19. Kurtzke, J.F. (1983). Rating neurologic impairment in multiple sclerosis: an expanded disability status scale (EDSS). *Neurology* 33, 1444–1452. <https://doi.org/10.1212/wnl.33.11.1444>.
20. Thompson, A.J., Banwell, B.L., Barkhof, F., Carroll, W.M., Coetzee, T., Comi, G., Correale, J., Fazekas, F., Filippi, M., Freedman, M.S., et al. (2018). Diagnosis of multiple sclerosis: 2017 revisions of the McDonald criteria. *Lancet Neurol.* 17, 162–173. [https://doi.org/10.1016/S1474-4422\(17\)30470-2](https://doi.org/10.1016/S1474-4422(17)30470-2).
21. Wijburg, M.T., Warnke, C., McGuigan, C., Koralnik, I.J., Barkhof, F., Killestein, J., and Wattjes, M.P. (2021). Pharmacovigilance during treatment of multiple sclerosis: early recognition of CNS complications. *J. Neurol. Neurosurg. Psychiatry* 92, 177–188. <https://doi.org/10.1136/jnnp-2020-324534>.
22. Geraldes, R., Ciccarelli, O., Barkhof, F., De Stefano, N., Enzinger, C., Filippi, M., Hofer, M., Paul, F., Preziosa, P., Rovira, A., et al. (2018). The current role of MRI in differentiating multiple sclerosis from its imaging mimics. *Nat. Rev. Neurol.* 14, 199–213. <https://doi.org/10.1038/nrneuro.2018.14>.
23. Kelley, B.J., and Rodriguez, M. (2009). Seizures in patients with multiple sclerosis: epidemiology, pathophysiology and management. *CNS Drugs* 23, 805–815. <https://doi.org/10.2165/11310900-000000000-00000>.
24. Neuß, F., von Podewils, F., Wang, Z.I., Süße, M., Zettl, U.K., and Grothe, M. (2021). Epileptic seizures in multiple sclerosis: prevalence, competing causes and diagnostic accuracy. *J. Neurol.* 268, 1721–1727. <https://doi.org/10.1007/s00415-020-10346-z>.
25. Jenkins, B., West, J.A., and Koulman, A. (2015). A review of odd-chain fatty acid metabolism and the role of pentadecanoic acid (c15:0) and heptadecanoic acid (c17:0) in health and disease. *Molecules* 20, 2425–2444. <https://doi.org/10.3390/molecules20022425>.
26. Jones, L.L., McDonald, D.A., and Borum, P.R. (2010). Acylcarnitines: role in brain. *Prog. Lipid Res.* 49, 61–75. <https://doi.org/10.1016/j.plipres.2009.08.004>.
27. Villoslada, P., Alonso, C., Agirrezabal, I., Kotelnikova, E., Zubizarreta, I., Puliido-Valdeolivas, I., Saiz, A., Comabella, M., Montalban, X., Villar, L., et al. (2017). Metabolomic signatures associated with disease severity in multiple sclerosis. *Neurol. Neuroimmunol. Neuroinflamm.* 4, e321. <https://doi.org/10.1212/NXI.0000000000000321>.
28. Kasakin, M.F., Rogachev, A.D., Predtechenskaya, E.V., Zaigraev, V.J., Koval, V.V., and Pokrovsky, A.G. (2020). Changes in amino acid and acylcarnitine plasma profiles for distinguishing patients with multiple sclerosis from healthy controls. *Mult. Scler. Int.* 2020, 9010937. <https://doi.org/10.1155/2020/9010937>.
29. Genchi, A., Brambilla, E., Sangalli, F., Radaelli, M., Bacigaluppi, M., Furlan, R., Andofo, A., Drago, D., Magagnotti, C., Scotti, G.M., et al. (2023). Neural stem cell transplantation in patients with progressive multiple

- sclerosis: an open-label, phase 1 study. *Nat. Med.* 29, 75–85. <https://doi.org/10.1038/s41591-022-02097-3>.
30. Dambrova, M., Makrecka-Kuka, M., Kuka, J., Vilskersts, R., Nordberg, D., Attwood, M.M., Smesny, S., Sen, Z.D., Guo, A.C., Oler, E., et al. (2022). Acylcarnitines: nomenclature, biomarkers, therapeutic potential, drug targets, and clinical trials. *Pharmacol. Rev.* 74, 506–551. <https://doi.org/10.1124/pharmrev.121.000408>.
 31. Tubridy, N., Coles, A.J., Molyneux, P., Compston, D.A., Barkhof, F., Thompson, A.J., McDonald, W.I., and Miller, D.H. (1998). Secondary progressive multiple sclerosis: the relationship between short-term MRI activity and clinical features. *Brain* 121, 225–231. <https://doi.org/10.1093/brain/121.2.225>.
 32. Vidal-Jordana, A., Sastre-Garriga, J., Pérez-Miralles, F., Tur, C., Tintoré, M., Horga, A., Auger, C., Río, J., Nos, C., Edo, M.C., et al. (2013). Early brain pseudoatrophy while on natalizumab therapy is due to white matter volume changes. *Mult. Scler.* 19, 1175–1181. <https://doi.org/10.1177/1352458512473190>.
 33. Gupta, N., Henry, R.G., Strober, J., Kang, S.M., Lim, D.A., Bucci, M., Caverzasi, E., Gaetano, L., Mandelli, M.L., Ryan, T., et al. (2012). Neural stem cell engraftment and myelination in the human brain. *Sci. Transl. Med.* 4, 155ra137. <https://doi.org/10.1126/scitranslmed.3004373>.
 34. Radoszkiewicz, K., Hribljan, V., Isakovic, J., Mitrecic, D., and Sarnowska, A. (2023). Critical points for optimizing long-term culture and neural differentiation capacity of rodent and human neural stem cells to facilitate translation into clinical settings. *Exp. Neurol.* 363, 114353. <https://doi.org/10.1016/j.expneurol.2023.114353>.
 35. Vescovi, A.L., Parati, E.A., Gritti, A., Poulin, P., Ferrario, M., Wanke, E., Frölichsthal-Schoeller, P., Cova, L., Arcellana-Panillo, M., Colombo, A., and Galli, R. (1999). Isolation and cloning of multipotential stem cells from the embryonic human CNS and establishment of transplantable human neural stem cell lines by epigenetic stimulation. *Exp Neurol* 156 (1), 71–83. <https://doi.org/10.1006/exnr.1998.6998>.
 36. Abercrombie, M. (1946). Estimation of nuclear population from microtome sections. *Anat. Rec.* 94, 239–247. <https://doi.org/10.1002/ar.1090940210>.
 37. Lublin, F.D., Reingold, S.C., Cohen, J.A., Cutter, G.R., Sorensen, P.S., Thompson, A.J., Wolinsky, J.S., Balcer, L.J., Banwell, B., Barkhof, F., et al. (2014). Defining the clinical course of multiple sclerosis: the 2013 revisions. *Neurology* 83, 278–286. <https://doi.org/10.1212/WNL.0000000000000560>.
 38. McDonald, W.I., Compston, A., Edan, G., Goodkin, D., Hartung, H.P., Lublin, F.D., McFarland, H.F., Paty, D.W., Polman, C.H., Reingold, S.C., et al. (2001). Recommended diagnostic criteria for multiple sclerosis: guidelines from the International Panel on the diagnosis of multiple sclerosis. *Ann. Neurol.* 50, 121–127. <https://doi.org/10.1002/ana.1032>.
 39. Burman, J., Raininko, R., Blennow, K., Zetterberg, H., Axelsson, M., and Malmstrom, C. (2016). YKL-40 is a CSF biomarker of intrathecal inflammation in secondary progressive multiple sclerosis. *J. Neuroimmunol.* 292, 52–57. <https://doi.org/10.1016/j.jneuroim.2016.01.013>.
 40. Nemkov, T., Reisz, J.A., Gehrke, S., Hansen, K.C., and D'Alessandro, A. (2019). High-throughput metabolomics: isocratic and gradient mass spectrometry-based methods. *Methods Mol. Biol.* 1978, 13–26. https://doi.org/10.1007/978-1-4939-9236-2_2.
 41. Nemkov, T., Hansen, K.C., and D'Alessandro, A. (2017). A three-minute method for high-throughput quantitative metabolomics and quantitative tracing experiments of central carbon and nitrogen pathways. *Rapid Commun. Mass Spectrom.* 31, 663–673. <https://doi.org/10.1002/rcm.7834>.
 42. Reisz, J.A., Zheng, C., D'Alessandro, A., and Nemkov, T. (2019). Untargeted and semi-targeted lipid analysis of biological samples using mass spectrometry-based metabolomics. *Methods Mol. Biol.* 1978, 121–135. https://doi.org/10.1007/978-1-4939-9236-2_8.
 43. Moraal, B., Wattjes, M.P., Geurts, J.J., Knol, D.L., van Schijndel, R.A., Pouwels, P.J., Vrenken, H., and Barkhof, F. (2010). Improved detection of active multiple sclerosis lesions: 3D subtraction imaging. *Radiology* 255, 154–163. <https://doi.org/10.1148/radiol.09090814>.
 44. Battaglini, M., Jenkinson, M., and De Stefano, N. (2012). Evaluating and reducing the impact of white matter lesions on brain volume measurements. *Hum. Brain Mapp.* 33, 2062–2071. <https://doi.org/10.1002/hbm.21344>.

STAR★METHODS

KEY RESOURCES TABLE

REAGENT or RESOURCE	SOURCE	IDENTIFIER
Antibodies		
Mouse Anti-Glial Fibrillary Acidic Protein Antibody	Merck Millipore	Cat# MAB3402; RRID:AB_94844
Mouse Anti-Galactocerebroside Antibody,	Merck Millipore	Cat# MAB342; RRID:AB_94857
Rabbit anti-Tubulin β -3 (TUBB3) Antibody	Biogen	Cat# 802001; RRID:AB_2564645
Mouse monoclonal anti-human nuclei (huN, 1:200)	Millipore	Cat# MAB1281; RRID:AB_94090
Rabbit anti-Ki67 (1:500)	Novus Biologicals	Cat# NB600-1252; RRID:AB_2142376
Rabbit polyclonal anti-doublecortin (DCX, 1:400)	Cell Signaling	Cat#4604S
Rabbit polyclonal anti-Glial Fibrillary Acidic Protein Antibody (GFAP, 1:500)	Agilent DAKO	Cat# Z0334; RRID:AB_10013382
Rabbit polyclonal anti-NG2 (1:50)	Millipore	Cat# AB5320; RRID:AB_11213678
Chemicals, peptides, and recombinant proteins		
GMP Recombinant human bFGF	Peprotech	Cat# GMP100-18B
GMP Recombinant human EGF	Peprotech	Cat# GMP100-15
DMEM/F12 10X	Thermo Scientific	Cat# 32500-035
Cultrex® Basement Membrane Extract,	Trevigen	Cat# 3434-001-02
Poli-L-lisina	Sigma Aldrich	Cat# P9155
Deposited data		
Metabolomics data	This paper	Metabolomics Workbench ID: ST002857 for CSF and Metabolomics Workbench ID: ST002858 for Serum
Experimental models: Cell lines		
Human fetal brain neural stem cells (animal studies and clinical trial)	Donor from Fondazione IRCCS Casa Sollievo della Sofferenza	hNSC 03/14b
Experimental models: Organisms/strains		
Mice, Hsd:Athymic Nude-Foxn1 ^{nu} , Female	Inotiv, Envigo	Cat# 408761
Software and algorithms		
SIENAx	www.fmrib.ox.ac.uk	v 2.6
SAS Release 9.4	SAS Institute, Cary, NC, USA.	Release 9.4
LipidSearch	Thermo Fisher	v.5.0 RRID:SCR_023716
El-Maven	Elucidata	v.0.12 RRID:SCR_022159
GraphPad Prism	http://www.graphpad.com/	v.7 RRID:SCR_002798
FMRIB Software Library (FSL)	www.fmrib.ox.ac.uk	v 5.0
3D Slicer	www.slicer.org	v.4.5.0
LST toolbox	Wellcome Centre for Human Neuroimaging	v 3.0

RESOURCE AVAILABILITY

Lead contact

Further information and requests for resources and reagents should be directed to and will be fulfilled by the lead contact, Angelo Luigi Vescovi (angelo.vescovi@unimib.it).

Materials availability

This study did not generate new unique reagents.

Data and code availability

Metabolomics data have been deposited and are publicly available through Metabolomics Workbench ID: ST002857, for CSF; and Metabolomics Workbench ID: ST002858 for Serum. This paper does not report original code. Any additional information required to re-analyse the data reported in this paper is available from the [lead contact](#) upon request, unless for the confidential medical records and related.

EXPERIMENTAL MODEL AND STUDY PARTICIPANT DETAILS

03/14b human Neural Stem Line

The ACT hNSC 03/14b line used in this study consists of a highly enriched population of hNSCs extracted from a single female foetal human donor resulting from a spontaneous miscarriage at 16 weeks after conception. The tissue was obtained in full compliance with the conditions and practices required by GMP regulations under the approval of the ethical committee of the Institute “Casa Sollievo della Sofferenza di San Pio da Pietrelcina”, with the donors’ parents’ informed consent. All specimen collection and medical procedures are in full accord to the Helsinki declaration (WMA Declaration of Helsinki - Ethical Principles for Medical Research Involving Human Subjects).

Extensive characterization of the cells used in this study, which involved the systematic delineation of their characteristics, antigenic properties, functional stability, differentiation capacity, engraftment ability in the adult CNS and potential tumorigenicity was performed as previously described.¹⁷

To produce the ACT hNSC 03/14b line starting from the foetal brain specimen, three main steps have been performed: *i) Primary culture*, *ii) Intermediate Product preparation and cryopreservation* *iii) Final Product formulation*.

(i) Primary culture

Human brain tissue was immediately transferred under strict sterile conditions to the GMP facility in a controlled environment. Then brain specimen was washed in a PBS solution (Dulbecco’s PBS 1X, Carlo Erba Reagent) supplemented with 50 µg/ml of gentamicin (only for this first step, to rinse the tissue) and mechanically dissociated to reach a monocellular suspension. Cells were seeded at a density of 10⁴ cells/cm² in a chemically defined culture medium and under the very same conditions that were described previously (Vescovi et al.³⁵). Cultures were maintained in a humidified incubator at 37°C, 5% O₂ and 5% CO₂ and cells were allowed to proliferate as free-floating clusters named neurospheres according to ‘*neurosphere assay technique*’. This technique allows to obtain a hNSCs culture with the very same characteristic independently from donor gestation age. At this stage, the cell culture is subjected to IPCs (In Process Controls): LAL test, Bact/Alert.

(ii) Intermediate Product preparation and cryopreservation

Approximately 7–10 days after the primary cell seeding, neurospheres were collected in 15 mL tube, centrifuged, the supernatant discharged, and the cell pellet mechanically dissociated. The obtained cell suspension was counted following the Eu.Ph ‘*Nucleated cell count*’ method, and cells were replated at the same initial density as described above in the same chemical defined medium. This *amplification step* (detailed in [method details](#)) was routinely repeated up to 10 times (with a minimum of 6 times) and the cells produced were counted at every passage. A graph reporting the variation of cell number along the time was generated to verify that the obtained *growth curve* (detailed in [method details](#)) had a positive slope. Throughout these passages aliquots of cells were frozen as neurospheres and cryopreserved in 10% DMSO (dimethyl sulfoxide) culture medium as a pharmaceutical intermediate product, with an assigned batch number according to an internal standard operating procedure that correlate donor to produced cell line hiding the donor generality. This freezing step is done in order to coordinate the timing of cell production with the surgery schedule and also to generate an ‘*Intermediate Product*’, to warrant the series of quality controls (*Release tests: Mycoplasma, sterility, LAL tes, Karyotype, SNP assay, Clonal Efficiency, Differentiation, Growth Factor Dependence, Growth Curve*) required to certify the safety, identity, potency and the pharmaceutical grade of the donor hNSCs. Batches of this Intermediate Product were also used for the non-clinical *in vivo* studies (see [method details](#)).

(iii) Final product formulation

Once the date of the surgery was determined, batches of the Intermediate Product were thawed, and cells underwent additional *amplification passages* (details in [method details](#)). At the last passage prior to the formulation of the “final product”, cells were allowed to grow for a shorter period before collection (24–96 hours instead of 7–10 days). This procedure represents a ‘*final selection step*’ that allows to enrich the final product (cell suspension) for highly immature, clonogenic cells. In fact, the more mature cells that constitute the 7-days-neurosphere are eliminated with the manual dissociation and are not re-generated within the short time window (24–96 hrs) before transplant. For the formulation of the final product cells were collected by centrifugation, cell counted and to suspended in sterile, endotoxin-free HBSS (Hank’s Balanced Salt Solution) to reach the correct viable cell concentration according to clinical protocol indications. HBSS absence of mycoplasmas, pH, sterility and osmolarity are routinely certified from the supplier. hNSCs were manipulate overall no more than 20 passages to minimize the risk of karyotype damage and in compliance with our drug process validation as authorized by AIFA. Release tests for the final product were Mycoplasma, Sterility, LAL Test, Karyotype, SNP assay, *Clonal Efficiency* (see [method details](#)), *Differentiation* (see [method details](#)), *Growth Factor Dependence*, *Growth curve evaluation*, *Viability evaluation*.

Animals safety study

Animal welfare

All animal procedures and protocols have been reviewed and authorized by the Institutional Animal Welfare Committee (OPBA) of University of Milano-Bicocca and by the Italian Ministry of Health (aut. Number: 751/2019-PR; and 651/2016-PR;). For animal studies on the ACT hNSC 03/14b line a total of $n = 17$ female mice (Hsd:Athymic Nude-Foxn1^{nu}, #408761, Envigo RMS SRL) were analysed. The age of animals at time of transplantation ranged between 5–8 weeks and the weight between 19–21 gr. Animals were allowed to acclimate for at least 1 week prior to transplant.

Animal housing

Animals were housed in ventilated rack cages (5 animals/cage) filled with autoclaved bedding. Irradiated Global Diet 2918 (Inotiv, Teklad Laboratory Animal Diet) and autoclaved water were provided *ad libitum*. Shredded paper was used for environmental enrichment. Environmental temperature and humidity were set between 20°C to 25°C and 40–60% and environmental light was provided according to a 12 hours:12 hours light:dark cycle.

Clinical trial design and patient selection

This was a Phase I safety study of human neural stem cell transplantation for the treatment of Secondary Progressive Multiple Sclerosis patients. A sample of 15 subjects with SPMS, who met eligibility criteria were enrolled. No control group was included. All subjects received intracerebroventricular injections of human Neural Stem Cells (03/14b). The trial was registered in ClinicalTrials.gov: NCT03282760. IRB approval granted by Ethical Committee section “IRCCS Istituto dei Tumori Giovanni Paolo II” Bari, Italy seconded at Fondazione Casa Sollievo della Sofferenza, San Giovanni Rotondo (Foggia) Italy. Details regarding Study Design and Inclusion and Exclusion Criteria are provided in [method details](#).

METHOD DETAILS

hNSC culture and characterization

Amplification step for ACT hNSC 03/14b

The vial of cell is thaw using a dry bath at 37°C for 5–10 minutes, transferred to a 15 ml tube with 5 ml of fresh medium, centrifuged for 10' at 192g. The supernatant is discarded, the cell pellet gently resuspended and the cells seeded in a 75 cm² plastic flask cell culture treated. Cells are incubated for 24–48 hours 5% O₂, 5% CO₂ and 37°C with >90% humidity. For the amplification step, the content of the flasks is collected by centrifugation as described and the supernatant is discarded with the exception of 50–100 μl. Using a 200 μl pipette with a sterile tip, the pellet is dissociated until obtaining a single cell suspension. Cells are counted using a Burker Chamber count cells and the viability evaluated using the standard trypan blue exclusion method. Cells are seeded at 10'000/cm² in 12 ml of pre-conditioned media using a 75 cm² flask and incubated at 5% O₂, 5% CO₂ and 37°C for 7–10 days monitoring their growth until they reach a diameter of 100 μm and can be expanded again.

Clonal efficiency test (CE index)

To verify the clonal efficiency of hNSCs, 100 μm-sized neurospheres were mechanically dissociated to obtain a single-cell suspension and seeded in 8 wells of a 24 flat-bottom wells plate (coated with 200 μl of Poly-L-lysine). Before seeding live cells, number was quantified using a Burker Chamber and the standard trypan blue exclusion method. Two cell suspensions were prepared (500 cells/ml and 250 cells/ml, respectively) and each suspension was seeded in four coated wells. Cells are then incubated at 5% O₂, 5% CO₂ and 37°C for 7 days. At the end, the number of spheres with diameter larger than 50 μm were counted. The % of clones was calculated as the ratio between the total cell seeded and the number of neurospheres obtained.

Differentiation test

For the differentiation test, 240.000 hNSCs were seeded in 16 ml of culture medium in the presence of the sole bFGF (without EGF), on top of round, sterile, glass coverslips (12 mm of diameter) disposed in 8 wells of a 24 flat-bottom wells plate and coated with Cultrex (200 μl/coverslip, incubated for 1 hour followed by aspiration of the unpolymerized Cultrex solution). Before seeding, neurospheres were mechanically dissociated to obtain a single-cells suspension (seeding concentration: 30.000 cells/2 ml/well and incubated at 5% O₂, 5% CO₂ and 37°C for 3 days. Medium was hence replaced with DMEM/F12 supplemented with 2% FBS, w/o growth factors and incubated for 7 days. At the end hNSCs were fixed with 1 ml of 4% paraformaldehyde for 1 hour and stored in 2 ml of PBS 1X at 2–8°C until immunostaining. The presence of neurons, astrocytes and oligodendrocytes in the progeny of hNSCs was evaluated by immunostaining with antibodies that recognize GFAP, TUBB-III and GalC.

Growth curve

Growth curve is the mathematic elaboration of the data obtained during cell culture; longer cultures allow to elaborate more precise curves. Five passages are the minimum number for a reliable growth curve. Using a spreadsheet editor graph the growth curve was obtained as indicated below:

For the abscissa was used the days of culture.

The ordinate for each passage (p) was determined with the following formula:

$$y(P) = \frac{c}{b} * y(P - 1)$$

Where: c represents the number of cells obtained; b represents the number of cells seeded at the previous passage; P is the number of the passage you are performing; $P-1$ represents the y determined for the previous passage (note: for the first passage y =number of seeded cells). The trendline of the graph was calculated and its slope was considered the indicator of the growth curve.

Animal studies: surgery, behavior, histology **Human NSC 03/14b preparation and injection**

For the animal safety studies batches from the Intermediate Product of 03/14b were used. The 03/14b were amplified and the passage before transplant were seeded in growth medium at a density of 10^4 cells/cm². 24-96 hrs later were collected and resuspended as single cells in HBSS (Gibco #14175095) at a density of 10^5 cells/ μ l.

On the day of cellular transplantation, athymic Foxn1^{nu} immune deficient mice, were anesthetized by intraperitoneal injection of 10ml/kg of a Ketamine/Xylazine solution (final dosage 30 mg/kg and 5 mg/kg). Before injections mice were positioned into the stereotaxic frame (Stoelting Lab Standard Stereotaxic) complemented with the Cunningham™ Mouse Adaptor. A manually controlled 5 μ l Hamilton syringe mounted onto the stereotaxic frame with a proper holder was used for hNSCs injection (Cemented needle, Gauge 30, length 1cm, point style 4 45°). Along surgery an eye ointment was added to prevent eye dryness (PureLube, Vet Ointment) and temperature of the mouse was controlled by using a heating pad. The skin was disinfected by Betadine solution and the skull exposed by performing a midline sagittal incision with a scalpel. The correct alignment of the head (*'flat-skull position'*) was assessed by measuring and matching the dorso-ventral coordinates of Bregma and Lambda suture under surgical microscope guidance (Zeiss). The coordinates to target the selected brain region (see below) were individuated under surgical microscope guidance: (i) to target the corpus striatum (ISI): 0,0 mm antero-posterior to the Bregma, 2.7 mm laterally to the sagittal suture; (ii) to target the lateral ventricle (ICVI): - 0.1 mm antero-posterior to the Bregma, 0.7 mm lateral to the sagittal suture.

The needle was introduced through a 2 mm diameter hole, performed in the skull by using a specific micro-drill under surgical microscope guidance to individuate the dura mater. Prior to hNSCs loading, the syringe has been flushed with HBSS solution and then loaded with 3 μ l of hNSCs suspension solution in HBSS (single cells resuspended to final concentration 1×10^5 cells/ μ l). The needle was positioned at the following dorso-ventral coordinates from dura mater (-2.7 mm for striatal injection and -2 mm for intraventricular injection). The cell suspension was finally manually injected at a rate 0.5 μ l/min. The syringe was retracted and the skin sutured and disinfected. Post-surgery, mice were allowed to recover on a heated pad.

Clinical surveillance of animal health

The animals were monitored weekly, up to 6 months after transplantation to detect neurological and behavioural signs of brain damage and/or tumour growth in the transplanted brain hemisphere.

The weekly check list included: (i) consistent weight loss (>20%); (ii) hydrocephalus (presence of deformation of the skull); (iii) motor deficits: ataxia (by observing if the animal maintains its balance/coordination while walking) or asymmetrical motor behaviour (after observation of the animal in an open field); (iv) presence of curvature of the spine (the mouse is allowed to walk freely and absence of kyphosis is recorded); (v) exophthalmos.

Immunohistological studies

For histological analyses, at 6 months post-transplant animals were euthanized by ketamine/xylazine anaesthesia followed by intracardial perfusion-fixation with physiological solution, followed by fixative solution (4% paraformaldehyde, Sigma #158127 in phosphate buffer). The animals' brains and organs (lungs, heart, intestine, kidneys, liver, and spleen) were macroscopically observed to identify gross morphological alterations or tumour masses (necropsy). Organs were removed, postfixed overnight, cryoprotected with sucrose solutions (10%, 20% and 30%, 24 hours each), embedded in OCT (Killik, Bio Optica, #05-9801) and frozen above liquid nitrogen vapors to perform histological analyses. Brains were micro-sectioned by cryostat to a thickness of 15–20 μ m and processed for histological staining (hematoxylin/eosin) to identify gross macroscopic alterations of ventricles or brain parenchyma. For survival and brain-biodistribution immunofluorescence analysis were performed using anti-human specific huN antibody to identify hNSCs (Zeiss Axioplan 2 imaging). All cells expressing huN were counted in serial sections (spaced by circa 150–200 μ m) spanning the graft area, the total number was calculated using Abercrombie correction³⁶ and expressed as the percentage over injected cells. To measure the antero-posterior migration distance we evaluated the distance in μ m between the first and last section of the brain containing transplanted cells for each animal. Brain biodistribution was evaluated by annotating on schematic brain coronal sections (derived from mouse brain atlas) the brain areas containing huN⁺ cells. Evaluation of hNSCs proliferation and cell phenotype were performed by identifying colocalization of huN marker with antibodies that recognize: Ki67 (proliferation marker), GFAP (astrocytes), DCX (migrating neuroblasts), TUBB3 (immature neurons) and NG2 (oligodendrocytes progenitors). Colocalization was assessed by confocal microscope (Leica DM IRE2 or NIKON A1R). Semi-quantitative evaluation of neural phenotypes was performed by counting the huN⁺ cells co-expressing each marker, in three serial sections of the brain (Zeiss Axioplan 2 or NIKON A1R, UniMib Microscopy platform). The values shown in [Figure 1](#) and [Table S1](#) represent the proportion of double-labelled cells over total huN⁺ cells in tissue sections. For each type of analysis $n \geq 3$ animals were evaluated, unless for NG2 ($n = 2$). Numbers in [Figure 1](#) and [Table S1](#) are as mean values \pm SEM.

Study design

Approval to the hNSC-SPMS study was granted by the Ethical Committees of Istituto Tumori 'Giovanni Paolo II' (Bari)/ 'Fondazione IRCCS Casa Sollievo della Sofferenza' Research Hospital (01PU/2016–21-01-2016), the 'Aziende Sanitarie dell'Umbria' (2404/17), Agenzia Italiana del Farmaco (AIFA), Istituto Superiore di Sanità (3090(16)-PRE21-1408–06-04-2016) and the study was registered

in the European Clinical Trials Database (EudraCT, 2015-004855-37), and in [ClinicalTrials.gov](https://clinicaltrials.gov): NCT03282760. All the patients signed the informed consent prior to study enrolment.

A total of 180 candidates volunteered between September 26, 2017, and January 13, 2020. The study was conducted in three centres. Two Italian centers, the 'IRCCS Casa Sollievo della Sofferenza' Research Hospital (*Site 1*) and the 'Santa Maria di Terni' Hospital (*Site 2*) recruited patients and performed the MRI examinations. The Multiple Sclerosis Centre of the Neurocentre of Southern Switzerland (*Site 3*) performed the magnetic resonance imaging (MRI) analysis. The ICVI of the ACT was performed at *Site 2*. Screening was done one month prior to enrolment in the study. The Run-in period started after the screening examination (Run-in-START) and lasted three months (Run-in-END). After screening in the two recruiting centres (as above), $n = 15$ subjects with active and non-active SPMS suffering from progressive disability were found to be eligible, consented, and were assigned a unique identification number. Participants, nine females and six males, had a mean age of 50 years (range: 38–57), and were recruited in similar proportions by the two study sites. The mean EDSS was 7.6 (range 7–8), mean disease duration was 23 years (range 14–30), and mean time from diagnosis to secondary progression was 10 years (range: 1–20).

The CONSORT diagram in [Figure S2](#) illustrates the recruitment protocol. The hNSC-SPMS study was advertised using the website of the hospitals and social media (eg Facebook and Twitter). The first patient selection was performed based on the documentation provided. Selected patients were then summoned in *Site 1* and *Site 2* (as above) for a first pre-screening meeting with the clinicians. Patients who agreed to participate were then subjected to the screening visit for the clinical trial. Following the surgical procedure, follow-up visits were performed monthly up to 12 months.

Before transplantation, all patients underwent the following examinations (at both Run-in-START and Run-in-END): physical and neurological exams; vital signs; pregnancy tests (in fertile women); haematological and urine tests; lumbar puncture for serum and CSF collection (stored at -80°C); John Cunningham Virus (JCV) testing; motor, sensory and visual evoked potentials; optical coherence tomography (OCT); Expanded Disability Status Score (EDSS); Multiple Sclerosis Functional Composite (MSFC)³⁷; Rao's brief repeatable battery (BRB) of neuropsychological tests; MS-QOL54 for the evaluation of quality of life; brain MRI. After the Run-in period, and if no serious co-morbidity nor health status changes occurred, the patients were eligible for the intervention. All patients were then randomly enrolled into four cohorts receiving four dosages (5, 10, 16, and 24M cells) of single donor, homogenous, foetal allogenic hNSC via ICVI according to a standard dose-escalation method that followed a modified Fibonacci sequence (100%, 60% and 50% dose increments). The flow chart in [Figure 2](#) illustrates the applied dose escalation method applying a standard phase I design with a 'Fibonacci' dose escalation scheme of 100%, 67%, 50%. Initial three patients were treated at the first dose level; if none of the 3 patients presented a SAE, the dose level was escalated one step for the next group of 3 patients, and the process continues as above. If 1 of the 3 patients presents SAE, 3 additional patients are treated at the current dose level. If none of these additional 3 patients showed a SAE, the dose level was escalated for the next cohort of 3 patients, and the process continued as above. Otherwise, the prior dose level is defined as the maximum tolerable dosage. Including 3 patients for each step and entering at least 6 patients in the last level dose, this design requires 15 to 24 patients.

The primary objective of the study was to assess the feasibility, safety, and tolerability of treatment by evaluating the mortality and the number and type of adverse events (AEs) leading to the maximum tolerated dose. The secondary objective was to evaluate the potential therapeutic effects of hNSCs by monitoring disease progression during the 12-month follow-up period.

Inclusion and exclusion criteria

Eligible patients were adults of either sex with a diagnosis of active or non-active SPMS with EDSS¹⁹ ≥ 6.5 and ≤ 8 , showing a progressive accumulation of disability after initial relapsing remitting course over the 2 years before recruitment (≥ 1.0 point for patients with EDSS = 6.5, and ≥ 0.5 points for patients with EDSS >6.5 , respectively) and ineligibility to other treatments (as assessed by the treating neurologist). Patients were excluded if: (i) suffering from psychiatric/personality disorders or severe cognitive decline; (ii) had an history of significant systemic, infectious, oncologic, or metabolic disorders or other autoimmune diseases; (iii) had chronic infections (HBV, HCV, HIV, tuberculosis); (iv) not able to undergo MRI scans; (v) received immunomodulant/immunosuppressive treatments <6 months before inclusion; (vi) participated in other research; (vii) had contra-indication to lumbar puncture or were pregnant or breastfeeding

hNSCs transplantation in people with SPMS

The ACT hNSC 03/14b line used in this study was produced following a previously described method,¹⁷ and in full compliance with the conditions and practices required by GMP regulations under Ethics Committee approval, with the donors' parents' informed consent and according to the Helsinki declaration. On the day of treatment, the hNSCs were collected from culture flasks, centrifuged, counted, and suspended in Hanks Balanced Salt Solution (HBSS) at a concentration of 50,000 cells/ μl . After batch release, the cells were maintained at $4 \pm 2^{\circ}\text{C}$ for up to 1.5 hours prior to implantation. Every batch of cells was tested for safety according to European Pharmacopoeia requirements for sterility, endotoxins level, mycoplasma, and karyotype stability. Non-compendial tests were performed for morphological and functional characterization. The standard panel test included: growth curve for safety and identity; growth factor dependence for safety and clonal efficiency for potency and identity assessment. The complete battery of quality controls for batch release, including post-surgery assays, was previously described,¹⁷ and it is also shown in [Figures S1](#) and [S3](#).

All patients were admitted to the Neurosurgery Unit of *Site 2* to undergo a single ICV injection of the ACT hNSCs 03/14b line. Thin-slice cranial CT or MRI scans were performed to evaluate the ventricular system and plan the procedure. A frameless stereotactic image guidance AxiEM system (Stealth station AxiEM electromagnetic tracking system, Medtronic navigation, Louisville, CO,

USA) was used to perform the ventricular cannulation. The correct catheter placement was verified based on the egress of CSF and a Rickham reservoir was then connected to it. After batch release, the ACT hNSCs 03/14b line were counted and suspended in HBSS at a concentration of 50,000 cells/ μ l and maintained at $4\pm 2^\circ\text{C}$ for up to 1.5 hours prior to implantation. All participants underwent CT scan within 24 hours from surgery to evaluate post-surgery complications and received oral methylprednisolone once (125 mg, 2 hours pre-intervention), intravenous cefazolin twice (1g, pre- and post-hNSC injection), and daily oral prednisone with a 28-day tapering (each week from 60, 40, 20, to 10 mg /day). Participants also received oral Tacrolimus (0.05 mg/kg, twice a day) 12 hours after the intervention and every 12 hours for the first 6 months. Tacrolimus was titrated to maintain blood levels within a 5–10 ng/ml range.

Outcome measures

To explore feasibility, safety, and tolerability of intracerebroventricular injections of the ACT hNSCs 03/14b line in subjects with active and non-active SPMS by investigating adverse events, general health status, and mortality. As secondary objectives we considered also functional disability, as measured by the EDSS and MSFC (MSFC includes the Timed 25-Foot Walk, T25W), PASAT3 and The 9-Hole Peg Test; MS relapses, measured by annualized relapse rate and time to confirmed relapse; cognitive functions, as measured by the RAO Brief Repeatable Battery of Neuropsychological Tests; Magnetic resonance Imaging (MRI) measures of lesion load, cortical atrophy, microstructural integrity and structural connectivity, and myelination. Neurophysiological parameters, explored with evoked potentials and optical coherence tomography (see also [Table S2](#)). To explore the impact of allogeneic hNSCs on MS-related, CSF and serum were biomarkers of neuronal loss and inflammation were evaluated by ELLA and SIMOA analysis.

Clinical and laboratory evaluation

Participants were followed for 12 months post-ICVI with monthly visits. Evaluations of health status and mortality were based on the occurrence of serious co-morbidities, changes in the general health, and the number of deaths due to the treatment (or to the procedure itself). All AEs were recorded and evaluated by the attending neurologists for any potential relationship with the ICVI of the ACT hNSC 03/14b line. Disease progression was monitored via EDSS, MFSC, annualised relapse rate and time to confirmed relapse, while cognitive function was assessed by Rao's Brief Repeatable battery (BRB). Clinical relapses were monitored and defined as (i) the appearance of a new neurologic deficit or (ii) the worsening of previously stable or improving pre-existing neurologic deficit, separated by at least 30 days from the onset of a preceding clinical demyelinating event.³⁸ The neurologic deficit must have been present for at least 24 hours and occurred in the absence of increased body temperature ($>37.5^\circ\text{C}$) or any known infection to be classified as clinical relapse. Of note, Covid pandemic, which partly occurred during our follow-up, did not disrupt the trial schedule, since some of the visits were performed virtually.

CSF and serum neurofilament (NfL) levels were used as markers of neurodegeneration/neuronal damage, while CHI3L1 (or YKL-40), as indicator of reactive astrocytes.³⁹

We also investigated serum and CSF levels of IL17A, IL2, IL8, TNFA, CCL2, CCL3, CX3CL1, VEGFA, OPN, and GFAP as exploratory objectives. For each one of these samples, we collected at least 6 ml of blood and 3 ml of CSF. The specimens were centrifuged at 2000g for 10 min, and 400g for 10 min respectively and divided into aliquots of 200 μ l or 500 μ l while working on ice. They were then immediately stored in a -80° ultra-freezer until the end of the trial. For quantification of IL17A, IL2, IL8, TNFA, CCL2, CCL3, CX3CL1, VEGFA, CHI3L1 and OPN, commercially available kits for the ELLA microfluidic system (Bio-Techne, Minneapolis, USA) were used and measurement performed according to the manufacturer's instructions. NfL and GFAP content was measured using SIMOA Technology according to the manufacturer's instructions (Quanterix Simoa® NF-light™ Advantage Kit).

Mass spectrometry-based metabolomics and lipidomics analysis

Sample preparation

Extraction of metabolites and lipids from cerebrospinal fluid (CSF) and serum was performed as follows: 40 μ L of sample was aliquoted into 2mL deep well plates followed by an addition of 360 μ L cold MeOH:MeCN:H₂O (5:3:2, v:v:v) for metabolomics or pure methanol for lipidomics. Plates were then placed on a shaker at 4°C and plate shaker was set to 400 RPM for 30 minutes. Insoluble material was pelleted by centrifugation (4000 RPM, 10 min) and supernatants were isolated for analysis by UHPLC-MS. All 96-well plate pipetting was done using Integra MINI 96 (Integra Biosciences).

Mass spectrometry metabolomics analysis

The Ultra-High Pressure Liquid Chromatography-Mass Spectrometry Metabolomics analysis employed a Vanquish UHPLC (Thermo Fisher Scientific) coupled to an Orbitrap Exploris 120 mass spectrometer (Thermo Fisher Scientific). 10 μ L injections of the samples were resolved across a 2.1 x 150 mm, 1.7 μ m particle size Kinetex SB-C18 column (Phenomenex) using a 5 minute, reversed-phase gradient as previously described.⁴⁰ The Exploris 120 was run independently in negative and positive ion mode, scanning in full MS mode from 65–975 m/z at 120,000 resolutions, with 50 Arb sheath gas, 10 Arb auxiliary gas, and 3 kV and 3.4 kV spray voltage for negative and positive modes, respectively. Calibration was performed prior to the run using the Easy-IC internal standard (Thermo Fisher Scientific). Run order of samples was randomized and technical replicates were injected after every 4 samples to assess quality control. Raw files were converted to .mzXML using RawConverter. The resultant files were processed with EI-Maven (Elucidata) alongside the KEGG database for metabolite assignment and peak integration as previously described.⁴¹

Lipidomics and Oxylipins analysis

The Ultra-High Pressure Liquid Chromatography-Mass Spectrometry Oxylipin analysis employed a Vanquish UHPLC system (Thermo Fisher Scientific) coupled to a Q Exactive mass spectrometer (Thermo Fisher Scientific). 10 μ L injections of the samples were resolved across a 2.1 x 100 mm, 1.7 μ m particle size Acquity UPLC BEH column (Waters) using a 7 minute, reversed-phase gradient. The mobile phases utilized were 20:80:0.02 acetonitrile:water:formic acid (v:v:v) and 20:80:0.02 acetonitrile:isopropyl alcohol:formic acid (v:v:v). The Q Exactive scanned in negative ion, full MS mode from 150-1500 m/z at 70,000 resolution. The method employed 45 Arb sheath gas, 15 Arb auxiliary gas, and 4 kV spray voltage. Calibration was performed prior to the run using the PierceTM Negative Ion Calibration Solution (Thermo Fisher Scientific). Raw files were converted to .mzXML using RawConverter. Run order of samples was randomized and technical replicates were injected after every 4 samples to assess quality control.

Lipidomics analysis employed a Vanquish UHPLC system (Thermo Fisher Scientific) coupled to a Q Exactive mass spectrometer (Thermo Fisher Scientific). 5 μ L injections of the samples were resolved across a 2.1 x 30 mm, 1.7 μ m particle size Kinetex C18 column (Phenomenex) using a 5 minute, reversed-phase gradient adapted from a previous method.⁴² The Q Exactive was run independently in positive and negative ion mode, scanning using data dependent MS2 (top 10) from 125-1500 m/z at 17,500 resolution, with 45 Arb sheath gas, 25 Arb auxiliary gas, and 4 kV spray voltage. Calibration was performed prior to the run using the PierceTM Positive and Negative Ion Calibration Solutions (Thermo Fisher Scientific). Run order of samples was randomized and technical replicates were injected after every 4 samples to assess quality control. Lipid assignments and peak integration were performed using LipidSearch v 5.0 (Thermo Fisher Scientific).

Magnetic resonance imaging (MRI)

Brain MRIs were performed at Run-in-START and Run-in-END, as well as during the 12-month follow up period to monitor structural changes related to intervention, disease activity and unexpected findings. MRIs were acquired at the two recruiting centres, using a Philips Ingenia scanner (Site 1, Philips Medical Systems, Best, The Netherlands) and a Siemens Verio scanner (Site 2, Siemens, Erlangen, Germany). The sequence types (3D-T2-FLAIR, 3D-T1-MPRAGE, T2 and T2* weighted, 3D-T1 post-contrast, and diffusion-weighted images) and parameters were harmonised between the two vendors to improve reproducibility. Analysis was performed at the Multiple Sclerosis Centre of the Neurocentre of Southern Switzerland (Site 3) aiming to detect (i) differences in lesion load between serial imaging and (ii) variations of brain parenchymal volume. Out of the 150 scheduled brain MRI examinations, 34 were missing, incomplete, or discarded for the following reasons: patient's refusal (n = 14), interrupted examination due to uncooperative patient (n = 13), examination performed elsewhere with a different protocol (n = 5), clinical status not allowing examination (n = 1); COVID pandemic emergency-related (n = 1). Immediately after acquisition, each MRI examination was assessed on-site for unexpected/acute findings requiring prompt action, by the local referring neuroradiologist. After data verification and anonymization, images were submitted to the Neurocenter of Southern Switzerland (Lugano, Switzerland) and reviewed by a neuroradiologist (E.P., with 14 years of experience) and a neurologist (C.G., with 22 years of experience) for quantification. Differences in lesion load between serial imaging were assessed to detect potential signal changes occurring in the brain after transplantation, including MS-unrelated changes. In 3 patients, Month 12 3D-FLAIR-T2 images were unavailable, thus the Month 6, Month 3 and Month 9 examinations were instead employed, respectively. The Run-in-END and the latest follow-up available 3D-FLAIR-T2 images were longitudinally compared by using a previously proposed, highly sensitive intensity subtraction method.⁴³ Difference images were calculated using an in-house developed script running under FSL v.5.0 (www.fmrib.ox.ac.uk) and 3D Slicer v.4.5.0 (www.slicer.org), according to the previously proposed method described in Moraal et al.⁴³ On these maps, new onset hyperintense changes are bright, as compared to the background medium-grey with no signal variation.⁴³ Highlighted findings were finally inspected and verified on source images. Once a brain change was detected, all available exams were retrospectively reviewed on a Philips Intellispace PC workstation, and the presence of contrast enhancement (if any) was recorded. To determine the degree of patients' MRI disease activity occurring before transplantation, the same procedure was also performed to compare the Run-in-START and Run-in-END examinations. Type 2 changes Monthly Lesion Activity Rate (MLAR) was estimated as: N (new and enlarging T2-visible lesions)/Months difference between time points. Changes in brain parenchymal volume were detected using the structural 3D-MPRAGE-T1 images of patients with both baseline (Run-in-END) and final follow-up (Month 12) time-points available. After excluding the three patients with unavailable Month 12 time-point MRI data (as above), and 2 additional patients for movement artefacts on the 3D-MPRAGE-T1 images, analyses were conducted on the remaining 10 patients. First, image lesion-filling⁴⁴ was performed using the LST v.3.0 toolbox, following lesion map check and manual refinement as needed. The T2-visible lesion volume was also estimated. Then, the baseline volume of the brain was calculated at Run-in-END. SIENAx v.2.6 (part of the FSL software suite) was employed to automatically estimate the normalized brain, grey matter, and white matter volumes (NBV, NGMV, NWMV). The percentage of parenchymal brain volume change (PBVC) between the Run-in-END and month 12 time-points was longitudinally estimated with SIENA v.2.6.

Data management and study monitoring

Trial demographic and clinical data were collected by designated investigators at the time of screening, run-in, and follow-up using ad-hoc electronic case report forms (e-CRFs). Data underwent reviews for source verification and systematic quality control. Additionally, data were reviewed periodically by an independent Data and Safety Monitoring Board (DSMB) to ensure protocol adherence, to monitor possible AEs, and for recommendations concerning the continuation, modification, or termination of the trial.

QUANTIFICATION AND STATISTICAL ANALYSIS

The demographic, clinical, and laboratory characteristics of the patients were reported as median and interquartile ranges (IQR) or as mean and standard deviation (SD), as appropriate, for continuous variables and as frequency and percentage for categorical variables. Normal distribution was checked using the Shapiro-Wilk test. Safety analyses were performed in all subjects. All AEs and severe AEs (SAEs) were recorded at follow-up visits and at the end of the study. Exploratory efficacy analyses were conducted in all subjects receiving at least one injection of hNSCs (here, FAS and ITT populations matched). Because the sample size was small and almost all the variables had non-normal distributions, pre/post differences (12-month visit vs end of Run-in visit) were assessed via linear models using ranks (with rank order as dependent variable). Test for linear trend from Run-In End to the end of the study were performed including into the models the time linear term. Within-time comparisons refer to the comparison of the outcome among the “dose-group” at the specified single time (visit). These comparisons were tested within the linear model specifying the “dose-group” contrasts at issues and the T-statistic test was used. Within-group comparisons refer to the comparison of the outcome between two time points (visits) within a specified single “dose-group”. These comparisons were tested within the linear model specifying the “time” contrasts at issues and the T-statistic test was used.

New or enlarging T2-visible lesions and lesions with contrast enhancement were analysed using negative binomial models with follow-up time as the offset and results reported as annualised rates. A p-value <0.05 was considered statistically significant. All analyses were performed using SAS Release 9.4, SAS Institute, Cary, NC, USA.

For the quality controls of the ACT 03/14b line (Figures S1 and S3) the data are represented as median±quartiles and statistical significance has been evaluated with One-Way ANOVA. For the non-clinical analyses (Figure 1; Table S1) data are represented as mean values±SEM and statistical significance has been evaluated with Mann-Whitney test.

Statistical analyses of metabolomics data, including two-way repeated measure ANOVA, hierarchical clustering analysis (HCA), linear discriminant analyses (LDA), network analysis of Spearman correlations and were performed using both MetaboAnalyst 5.0. Line plots were generated with an in-house developed code in R (4.2.3 2023-03-15).

ADDITIONAL RESOURCES

The Clinical Trial has been entered in the European Union Drug Regulating Authorities Clinical Trials Database (registry number: EudraCT 2015-004855-37), and in the NIH database ([ClinicalTrials.gov](https://clinicaltrials.gov): NCT03282760)